THE JOURNAL OF BIOLOGICAL CHEMISTRY VOL. 287, NO. 3, pp. 2221–2236, January 13, 2012

Yeast Lipin 1 Orthologue Pah1p Regulates Vacuole Homeostasis and Membrane Fusion*

Received for publication, October 25, 2011, and in revised form, Novmeber 20, 2011 Published, JBC Papers in Press, November 25, 2011, DOI 10.1074/jbc.M111.317420

Terry Sasser[1], Quan-Sheng Qiu[1,2], Surya Karunakaran[1], Mark Padolina, Anna Reyes, Blake Flood, Sheena Smith, Chad Gonzales, and Rutilio A. Fratti[3]

From the Department of Biochemistry, University of Illinois at Urbana-Champaign, Urbana, Illinois 61801

Background: Pah1p is a phosphatidic acid phosphatase that generates diacylglycerol.
Results: Deletion of *PAH1* alters the sorting of fusion factors to the vacuole and inhibits fusion.
Conclusion: Conversion of phosphatidic acid to diacylglycerol is integral to vacuole homeostasis.
Significance: This is the first report that links a Lipin 1 homologue to the recruitment and activation of a Rab GTPase or the sorting of SNARE proteins.

Vacuole homotypic fusion requires a group of regulatory lipids that includes diacylglycerol, a fusogenic lipid that is produced through multiple metabolic pathways including the dephosphorylation of phosphatidic acid (PA). Here we examined the relationship between membrane fusion and PA phosphatase activity. Pah1p is the single yeast homologue of the Lipin family of PA phosphatases. Deletion of *PAH1* was sufficient to cause marked vacuole fragmentation and abolish vacuole fusion. The function of Pah1p solely depended on its phosphatase activity as complementation studies showed that wild type Pah1p restored fusion, whereas the phosphatase dead mutant Pah1p^{D398E} had no effect. We discovered that the lack of PA phosphatase activity blocked fusion by inhibiting the binding of SNAREs to Sec18p, an *N*-ethylmaleimide-sensitive factor homologue responsible for priming inactive *cis*-SNARE complexes. In addition, *pah1*Δ vacuoles were devoid of the late endosome/vacuolar Rab Ypt7p, the phosphatidylinositol 3-kinase Vps34p, and Vps39p, a subunit of the HOPS (homotypic fusion and vacuole protein sorting) tethering complex, all of which are required for vacuole fusion. The lack of Vps34p resulted in the absence of phosphatidylinositol 3-phosphate, a lipid required for SNARE activity and vacuole fusion. These findings demonstrate that Pah1p and PA phosphatase activity are critical for vacuole homeostasis and fusion.

Eukaryotic cells are compartmentalized by membrane-bound organelles that communicate through the trafficking of transport vesicles. The transport of cargo between organelles as well as between the plasma membrane and organelles requires a series of trafficking events that culminates in the fusion of membranes and mixture of lumenal contents. The mechanisms and machinery that drive membrane fusion are conserved from single cell eukaryotes to metazoans (1). We use vacuolar lysosomes from the yeast *Saccharomyces cerevisiae* to examine the regulation of vesicle fusion. Vacuole fusion requires many factors including three Q-SNAREs[4] (Vam3p, Vit1p, and Vam7p), one R-SNARE (Nyv1p), and the SNARE priming machinery Sec17p (α-soluble NSF attachment protein) and Sec18p (NSF). Fusion also requires the Rab GTPase Ypt7p, the effector complex HOPS, and regulatory lipids that include phosphoinositides, ergosterol, and DAG (2–4).

Vacuole fusion occurs through a series of stages that begins with priming when *cis*-SNARE complexes bound to Sec17p are disassembled by Sec18p, causing the release of Sec17p and the soluble SNARE Vam7p from the membrane (5, 6). During Ypt7p-dependent tethering/docking, Vam7p rebinds the membrane through its Phox homology domain that interacts with HOPS and phosphatidylinositol 3-phosphate (PI3P) (5, 7–9). Next, SNAREs form *trans*-complexes across the docking junction (10), stimulating the release of luminal calcium stores (11). During the tethering/docking stages vacuoles form three distinct morphological features. Vacuoles become tightly associated and form two flattened membrane discs termed the "boundary membrane." Proteins and lipids that mediate fusion become enriched at the boundary perimeter, termed the "vertex ring" (2, 12, 13).

Lipid metabolism is critical for the assembly and function of the vertex ring and is essential for membrane fusion (2–5, 14, 15). However, little has been reported on the role of individual metabolic reactions during fusion. Here we examined the role of phosphatidic acid (PA) dephosphorylation to form DAG. The importance of DAG and PA has been recently highlighted in several trafficking pathways. DAG is important for the formation of COP-I vesicles in retrograde traffic from the Golgi to

* This work was supported in part by March of Dimes Birth Defects Foundation Basil O'Connor Starter Scholar Research Award Grant 5-FY09-117 (to R. A. F.) and startup funds provided by the University of Illinois at Urbana-Champaign (to R. A. F.).

[1] These authors contributed equally to this work.

[2] Present address: School of Life Sciences, Lanzhou University, Lanzhou, 730000, China.

[3] To whom correspondence should be addressed: Dept. of Biochemistry, University of Illinois at Urbana-Champaign, 419 Roger Adams Laboratory, B-4, 600 S. Mathews Ave., Urbana, IL 61801. Tel.: 217-244-5513; Fax.: 217-244-5858; E-mail: rfratti@illinois.edu.

[4] The abbreviations used are: SNARE, soluble *N*-ethylmaleimide-sensitive factor attachment protein receptors; CBP, calmodulin-binding peptide; CORVET, class C core vacuole/endosome tethering; DAG, diacylglycerol; HOPS, homotypic fusion and vacuole protein sorting complex; NSF, *N*-ethylmaleimide-sensitive factor; PA, phosphatidic acid; PI, phosphatidylinositol; PI3P, phosphatidylinositol 3-phosphate; PAP, PA phosphatase; YPD, yeast extract/peptone/dextrose; Rh-PE, rhodamine phosphatidylethanolamine.

TABLE 1
Yeast strains used in this study

Strain	Genotype	Source
BJ3505	*MATα pep4::HIS3 prb1-Δ1.6R his3-200 lys2-801 trp1Δ101 (gal3) ura3-52 gal2 can1*	(42)
DKY6281	*MATα pho8::TRP1 leu2-3 leu2-112 ura3-52 his3-Δ200 trp1-Δ901 lys2-801*	(43)
DKY6281 *nyv1*Δ	DKY6281, *nyv1*Δ*::HIS5*	(36)
BJ3505 CBP-Vam3 *nyv1*Δ	BJ3505, *CBP-VAM3::Kan*^{r} *nyv1*Δ*::nat*^{r}	(44)
BJ3505 CBP-Vam3	BJ3505, *CBP-VAM3::Kan*^{r}	(44)
GFP-Ypt7	BJ3505	(12)
RFY17	BJ3505, *pah1*Δ*::Kan*^{r}	This study
RFY18	DKY6281, *pah*Δ*::Kan*^{r}	This study
RFY19	RFY17, *PAH1::3XHA*	This study
RFY20	RFY18, *PAH1::3XHA*	This study
RFY21	RFY17, *PAH1*^{D398E}*::3XHA*	This study
RFY22	RFY18, *PAH1*^{D398E}*::3XHA*	This study
RFY23	BJ3505, *dpp1*Δ*::URA3*	This study
RFY24	DKY6281, *dpp1*Δ*::URA3*	This study
RFY25	BJ3505, *lpp1*Δ*::URA3*	This study
RFY26	DKY6281, *lpp1*Δ*::URA3*	This study
RFY27	DKY6281, *PAH1::GFP*	This study

the endoplasmic reticulum (16) as well as tubulation within the Golgi apparatus (17). PA also plays an important role in SNARE activation during sporulation (18, 19), mitochondrial fusion (20), and exocytosis (21). Formation of both PA and DAG occurs through multiple metabolic pathways. In many studies the generation of PA and DAG is studied in the context of phospholipase activities. PA is the product of phospholipase D activity on phosphatidylcholine, whereas phospholipase C variants hydrolyze either phosphatidylcholine or phosphatidylinositol 4,5-bisphosphate to produce DAG. Furthermore, PA and DAG can be interconverted by DAG kinase and PA phosphatases. Although many studies have focused on phospholipase C and phospholipase D activity in the context of membrane trafficking, little is known about the importance of interconverting DAG and PA during membrane fusion. For this reason in this study we examined the role of PA phosphatase activity in vacuole fusion.

The importance of PA phosphatase (PAP) activity in vacuole homeostasis had not been thoroughly explored. *S. cerevisiae* contains three PAPs. Lpp1p is a polytopic PAP localized to Golgi puncta and dephosphorylates PA, lysophosphatidic acid, and DAG pyrophosphate via a Mg^{2+}-independent mechanism (22). Dpp1p is a Zn^{2+}-regulated seven-transmembrane domain PAP localized to the vacuole and acts on DAG pyrophosphate and PA (23). The soluble PAP Pah1p only hydrolyzes PA in a Mg^{2+}-dependent manner (24). Although all three PAPs can hydrolyze PA, Pah1p is the principal producer of DAG from PA (24). Mutations in the *PAH1* homologue *LPIN1* have been identified as the cause of fatty liver dystrophy and termed an "obesity" gene (25). WT Lipin 1 functions in glucose metabolism (26) and in the regulation of insulin levels (26, 27). Furthermore, mutations in Lipin 1 have been shown to lead to obesity by reducing fatty acid oxidation and energy expenditure (28) and may lead to severe consequences such as the onset of insulin resistance, a hallmark of adult obesity and type 2 diabetes.

Pah1p is a Mg^{2+}-dependent soluble 95-kDa protein with a central catalytic motif and an N-terminal amphipathic helix (29). The PA phosphatase activity of Pah1p is constitutive; however, its association with membranes and subsequent enzymatic activity is controlled through its state of phosphorylation. Phosphorylated Pah1p is soluble and present in the cytoplasm, whereas dephosphorylated Pah1p localizes to membranes and functions as a PA phosphatase (30). Pah1p is phosphorylated by the cyclin-dependent kinase Cdc28p and dephosphorylated by the membrane-anchored Nem1p-Spo7p phosphatase complex (31, 32). The association of Pah1p with membranes is mediated by an N-terminal amphipathic helix (33) that once dephosphorylated can bind to membranes, and deletion of the helix prevents catalytically active Pah1p from acting on its substrate. Although most of the membrane-bound Pah1p is found on the endoplasmic reticulum, active Pah1p can bind to other membranes, including lipid droplets, or artificial liposomes (30, 33, 34).

Pah1p plays a critical role in regulating the overall synthesis of lipids. When Pah1p is phosphorylated it indirectly regulates the expression of phospholipid synthesis genes (35). Phosphorylated Pah1p translocates to the nucleus where it regulates *INO1* for the production of lipids. This is critical during mitosis when the nuclear envelope and endoplasmic reticulum have to expand to replicate the organelles for daughter cells. Unphosphorylated Pah1p generates DAG, which can feed into the synthesis of triacylglycerol, phosphatidylcholine, and phosphatidylethanolamine (24). Deletion of *PAH1* leads to an accumulation PA and depletion of DAG and triacylglycerol.

EXPERIMENTAL PROCEDURES

Reagents—Reagents were dissolved in PS buffer (20 mM PIPES-KOH, pH 6.8, 200 mM sorbitol). Anti-Vam3p (36), anti-Sec18p (6), anti-Ypt7p (8), anti-Vps33p (37), GST-FYVE (38), His6-Gyp1–46p (13), Gdi1p (39), MARCKS effector domain (2), and GST-Vam7p (WT, Q283R and Y42A) (40, 41) were described previously. Propranolol, atenolol, and acebutolol were from Sigma and dissolved in PS buffer.

Strains—BJ3505 and DKY6281 were used for fusion assays (42, 43) (Table 1). BJ3505 calmodulin binding peptide (CBP)-Vam3p *nyv1*Δ was used for *trans*-SNARE complex isolation (44). BJ3505 CBP-Vam3p harboring Nyv1p was used for Sec18p-SNARE complex isolation. *PAH1* was deleted by homologous recombination with the kanMX6 cassette using PCR products amplified from pFA6a-kanMX6 (45) with homology flanking the *PAH1* coding sequences with the primers 5′-PAH1-KO and 3′-PAH1-KO (Table 2). The PCR product was transformed by standard lithium acetate methods into BJ3505 and DKY6281 to generate RFY17 and RFY18, respec-

TABLE 2
Primers used in this study

Oligonucleotide	Sequence
5′-PAH1-KO	5′-ACAGGGAAGAAATTACTGAAGATAGACACATCGGTCGAT TCGGATCCCCGGGTTAATTAA-3′
3′ PAH1-KO	5′-AGTATGGATCGTTATAAATAATATTCGGCTACAAGAATCT GAATTCGAGCTCGTTTAAAC-3′.
5′-DPP1-KO	5′-TATATATAGATAGAAACCCAACGTTGGATAACCTCACGA CAGATTGTACTGAGAGTGCAC-3′
3′ DPP1-KO	5′-GTCATCTTTATGTAATCGCTGTTATTCCATACAGAACAAT CTGTGCGGTATTTCACACCG-3′
5′-LPP1-KO-BJ3505	5′-AATCAAGGTCTGTTATCGTGGCTATTGCTCTAATTCATTA ATAGGCCACTAGTGGATCTG-3′
3′ LPP1-KO-BJ3505	5′-CTTATATAATAGAGCAAAGCTCGCCAGTGCTCCAGTTGT TTCAGCTGAAGCTTCGTACGC-3′
5′-LPP1-KO-DKY6281	5′-CTTATATGTAGTTTACATTTAATCAAGGTCTGTTATCGTG AGATTGTACTGAGAGTGCAC-3′
3′ LPP1-KO-DKY6281	5′-CTTATATAATAGAGCAAAGCTCGCCAGTGCTCCAGTTGTT CTGTGCGGTATTTCACACCG-3
5′-PAH1-GFP	5′-ATTCGATGACGATGAATTCGACGAAGATGAATTCGAAGA TCGGATCCCCGGGTTAATTAA-3
3′ PAH1-GFP	5′-AGTATGGATCGTTATAAATAATATTCGGCTACAAGAATC TGAATTCGAGCTCGTTTAAAC-3′

tively. Transformants were selected using YPD media containing G418. For complementation experiments, WT *PAH1* and *PAH1*^{D398E}, were subcloned from pGH312 and pGH312-D398E plasmids (46) (a gift from G. Carman, Rutgers University) into YEp352 using XbaI and SphI. RFY17 and RFY18 were transformed with p*PAH1* or p*PAH1*^{D398E} to generate RFY19–22. Transformants were selected using complete synthetic media lacking uracil. *DPP1* was deleted with the *URA3* cassette using PCR products amplified form pRS406 with homology flanking the *DPP1* open reading frame with the primers 5′-DPP1-KO and 3′-DPP1-KO. The PCR products were transformed into BJ3505 and DKY6281 to generate RFY23 and RFY24. *LPP1* was deleted using the hphMX4 or *URA3* cassettes using PCR products amplified form pAG32 or pRS406, respectively, with homology flanking the *LPP1* open reading frame with the primers 5′-LPP1-KO-BJ3505 and 3′-LPP1-KO-BJ3505 or 5′-LPP1-KO-DKY6281 and 3′-LPP1-KO-DKY6281 (45, 47). The PCR products were transformed into BJ3505 and DKY6281 to generate RFY25 and RFY26. For vacuole localization studies, *PAH1* was fused in-frame to GFP by homologous recombination. DKY6281 was transformed with a PCR product amplified from pFA6a-GFP(S65T)-kanMX6 with the primers 5′-PAH1-GFP and 3′-PAH1-GFP with homology flanking the stop codon of the *PAH1* gene to make RFY27 (48).

Vacuole Isolation and Content Mixing Fusion Assay—Vacuoles were isolated by floatation as described (43). *In vitro* content mixing fusion reactions (30 μl) contained 3 μg each of vacuoles from BJ3505 and DKY6281 backgrounds, fusion reaction buffer (20 mM PIPES-KOH, pH 6.8, 200 mM sorbitol, 125 mM KCl, 5 mM $MgCl_2$), ATP regenerating system (1 mM ATP, 0.1 mg/ml creatine kinase, 29 mM creatine phosphate), 10 μM coenzyme A, and 283 nM IB_2 (inhibitor of protease B). Reactions were incubated at 27 °C, and Pho8p activity was assayed in 250 mM Tris-Cl, pH 8.5, 0.4% Triton X-100, 10 mM $MgCl_2$, and 1 mM *p*-nitrophenyl phosphate. Fusion units were measured by determining the *p*-nitrophenolate-produced $min^{-1}\cdot\mu g^{-1}$ *pep4*Δ vacuole. *p*-Nitrophenolate absorbance was measured at 400 nm.

Microsomes were prepared as described (49). WT and *pah1*Δ cultures were grown in YPD, washed with PBS, and suspended in lysis buffer (10 mM Tris-Cl, pH 7.4, 300 mM sorbitol, 100 mM NaCl, 5 mM $MgCl_2$) with protease inhibitors (1 mM PMSF, 10 μM Pefabloc-SC, 5 μM pepstatin A, and 1 μM leupeptin). Cells were disrupted with glass beads by cycles of vortexing and cooling on ice. Lysates were centrifuged to pellet large debris, and supernatants were transferred to ultracentrifuge tubes. A total membrane fraction was collected by centrifugation (100,000 × *g*, 1 h, 4 °C) and resuspended in buffer (20 mM HEPES-KOH, pH 7.4, with protease inhibitors).

Lipid Mixing Fusion Assay—Lipid mixing assays were conducted using rhodamine phosphatidylethanolamine (Rh-PE; Invitrogen) as described with minor modifications (50). Briefly, BJ3505 background vacuoles (300 μg) were incubated in 400 μl of PS buffer containing 150 μM Rh-PE (10 min, 4 °C, nutating). Samples were mixed with 15% Ficoll in PS buffer (w/v) and transferred to a polyallomer ultracentrifuge tube. Samples were overlaid with 1.0 ml each of 8, 4, and 0% Ficoll. Labeled vacuoles were re-isolated by centrifugation using a Beckman SW60 Ti rotor (105,200 *g*, 30 min, 4 °C) and recovered from the 0–4%-Ficoll interface. Lipid mixing assays (90 μl) contained 2 μg of Rh-PE-labeled vacuoles and 16 μg of unlabeled vacuoles in fusion buffer. Reaction mixtures were transferred to a black, half-volume 96-well flat-bottom microtiter plate with nonbinding surface (Corning). Rhodamine fluorescence (λ_{ex} = 544 nm; λ_{em} = 590 nm) was measured using a POLARstar Omega fluorescence plate reader (BMG Labtech) at 27 °C. Measurements were taken every min for 75 min, yielding fluorescence values at the onset (F_0) and during the reaction (F_t). The final 10 measurements of a sample were taken after adding 0.33% (v/v) Triton X-100, averaged, and used as a value for the fluorescence after infinite dilution (F_{TX100}). The relative total fluorescence change $\Delta F_t/F_{TX100} = (F_t - F_0)/F_{TX100}$ was calculated.

Sec18p-SNARE Complex Detection—Analysis of Sec18p binding to *cis*-SNARE complexes was conducted using a modified *trans*-SNARE complex isolation assay (44, 50). For this assay we used vacuoles from BJ3505-CBP-Vam3p (*CBP-VAM3 NYV1*). The isolation of *cis*-SNARE-bound Sec18p was performed using 16× large-scale reactions (480 μl) containing 96 μg of vacuoles and incubated at 27 °C for 5 or 10 min and treated with buffer, propranolol, or anti-Sec18p to inhibit priming. Separate reactions were kept on ice as 0 min samples. After incubating, reactions were placed on ice for 5 min, and 30-μl samples were withdrawn from each reaction to assay Pho8p activity. The remaining 450-μl samples were centrifuged (13,000 × *g*, 15 min, 4 °C), and the supernatants were decanted. Vacuole pellets were overlaid with 200 μl of ice-cold solubilization buffer (20 mM Tris-Cl, pH 7.5, 150 mM NaCl, 1 mM $MgCl_2$, 0.5% Nonidet P-40 alternative, 10% glycerol) with protease inhibitors (0.46 μg/ml leupeptin, 3.5 μg/ml pepstatin, 2.4 μg/ml Pefabloc-SC, 1 mM PMSF) and gently resuspended. Solubilization buffer was added to a final volume of 600 μl, and extracts were mixed (20 min, 4 °C, nutating). Detergent-insoluble debris was removed by centrifugation (16,000 *g*, 20 min, 4 °C). Supernatants were transferred to fresh tubes, and 10% of

the extract was removed for input samples. The remaining extracts were brought to 2 mM $CaCl_2$. CBP-Vam3p complexes were incubated with 50 μl of equilibrated calmodulin-Sepharose 4B (GE Healthcare) (4 °C, 12 h, nutating). Beads were collected by centrifugation (4,000 *g*, 2 min, 4 °C) and suspended 4 times with the solubilization buffer followed by bead sedimentation. Bound proteins were eluted with SDS sample buffer containing 5 mM EGTA and heated at 95 °C for 5 min. The samples were resolved by SDS-PAGE, transferred to nitrocellulose, and probed by immunoblotting. Goat anti-rabbit secondary antibody conjugated to alkaline phosphatase (Pierce) was used with enhanced chemifluorescence substrate (GE Healthcare). Images were acquired using a Storm PhosphorImager 840 (Molecular Dynamics).

Trans-SNARE Complex Assay—The method for detecting *trans*-SNARE complexes is essentially identical to that of Sec18p-SNARE complex isolation with one modification. In the *trans*-SNARE assembly assay, we used vacuoles that lack *NYV1* and contain CBP-Vam3p on the same membrane (*CBP-VAM3 nyv1*Δ). These vacuoles were incubated with WT DKY6281 (*VAM3 NYV1*) for 60 min and processed for CBP-Vam3p isolation as described above.

GST-Vam7 Pulldown—GST-Vam7p-protein complex isolation was performed as described (40, 41). Briefly, large-scale 6× fusion reactions (180 μl) were incubated with 85 μg/ml anti-Sec17p IgG to block priming. After 15 min, anti-Vam3p IgG was added to selected reactions and incubated for an additional 5 min, adding buffer or 400 nM GST-Vam7p. After a total of 90 min, reactions were placed on ice for 5 min, and 30-μl aliquots were removed to measure fusion activity. The remaining vacuoles were re-isolated by centrifugation (11,000 × *g*, 10 min, 4 °C), and the supernatants were decanted before extracting vacuoles with solubilization buffer (20 mM HEPES-KOH, pH 7.4, 100 mM NaCl, 2 mM EDTA, 20% glycerol, 0.5% Triton X-100, 1 mM DTT) with protease inhibitors (1 mM PMSF, 10 μM Pefabloc-SC, 5 μM pepstatin A, and 1 μM leupeptin). Vacuole pellets were gently resuspended with 200 μl of solubilization buffer and incubation for 20 min on ice. Insoluble debris was sedimented by centrifugation (16,000 *g*, 10 min, 4 °C), and 176 μl of supernatants were transferred to new chilled tubes. Next, 16 μl was removed from each reaction as 10% total samples, mixed with SDS loading buffer, and heated (95 °C, 5 min). The remaining extracts were incubated with 30 μl of equilibrated glutathione-Sepharose 4B beads (GE Healthcare) (12 h, 4 °C, nutating). Beads were sedimented (3,000 rpm, 2 min, 4 °C) and washed with 1 ml solubilization buffer five times, and bound material was eluted with SDS loading buffer. Protein complexes were examined by Western blotting.

PA Phosphatase Activity—To examine native PAP activity on isolated vacuoles, we used thin layer chromatography (TLC). Isolated vacuoles were incubated with PA that was covalently tagged with the fluorescent molecule NBD. In this assay short chain Di-C6-NBD PA (0.4 μg; Avanti Polarlipids) was incubated with 3 μg of isolated vacuoles and treated with propranolol. This was carried out in reaction buffer (50 mM HEPES-KOH, pH 7.4, 200 mM sorbitol 100 mM NaCl, and 0.5 mg/ml BSA) and the ATP regenerating system. Reactions were incubated for 30 min at 30 °C. Lipids were extracted as described with some modification (51). Before extractions, three freeze-thaw cycles were performed using a 95 °C dry-bath and −80 °C freezer. Reactions were phase-extracted with a monophase of chloroform/methanol/water (2:1:0.8). Next, 1 ml each of chloroform and 1 M HCl were added to form two phases. The lower organic phase was removed and dried under an N_2 stream. Dried reactions were resuspended in 10 μl chloroform and spotted on to glass backed TLC plates (K6 silica gel; Whatman). Lipids were resolved in chloroform/methanol/acetone/acetic acid/water (53:10.5:21:10.5:3) and air-dried. Fluorescence was visualized using a Storm PhosphorImager 8400 with an excitation of 450 nm and emission of 520 nm.

Vacuole Docking—Vacuoles were purified from Pah1p-GFP, *pah1*Δ (RFY18), or DKY8281 strains and used in docking assays as previously described (2). Docking reactions contained 6 μg of vacuoles in 30 μl of docking reaction buffer (100 mM KCl, 0.5 mM $MgCl_2$, 20 mM Pipes-KOH, pH 6.8, 200 mM sorbitol), ATP regenerating system (0.3 mM ATP, 6 mM creatine phosphate, 0.7 mg/ml creatine kinase), 20 μM coenzyme A, and 283 nM IB_2 (inhibitor of protease B). After incubation (30 min, 27 °C), reactions were placed on ice, and vacuoles were stained with either 3 μM FM4-64 or 1 μM PSS-380. Where indicated, PI3P was detected with 0.2 μM Cy5-FYVE domain. Vacuoles were then mixed with 50 μl of 0.6% agarose in PS buffer and vortexed (3 s, medium setting), and 15-μl samples were mounted on slides and observed by fluorescence microscopy.

Ratiometric Quantitation—For ratiometric measurements of Cy5-FYVE localization, the maximum pixel values for vertex and outer edge membrane were measured for specific and nonspecific probes in each fluorescence channel as described (2). All vertices and outer edge membranes were measured within a vacuole cluster. In each experiment 15–20 clusters containing 100–300 vertices were analyzed for each treatment in multiple experiments. The data are presented in a representative experiment. First, pixel ratios of vertex-to-outer edge membrane were taken for each fluorescent channel. Pixel ratios for nonspecific labeling were normalized to 1. Next, ratios of specific-to-nonspecific labels were taken at each vertex and outer edge membranes, and enrichment was expressed relative to outer edge membrane intensities.

Whole Cell Imaging—Vacuole morphology was monitored by incubating yeast cells in YPD broth containing 5 μM FM4-64. Cultures (5 ml) were grown for 1 h in YPD with FM4-64 at 30 °C, washed with PBS, and chased for 3 h with fresh YPD alone. After incubation, the cells were concentrated by centrifugation, resuspended in 50 μl of PBS, mixed with 50 μl 0.6% agarose, and mounted (15 μl) on glass slides for observation. Images were acquired using a Zeiss Axio Observer Z1 inverted microscope equipped with a X-Cite 120XL light source, Plan Apochromat 63× oil objective (NA 1.4), and a AxioCam CCD camera.

RESULTS

Phosphatidic Acid Phosphatase Activity Is Required for Vacuole Homeostasis and Fusion—Vacuole fusion requires multiple regulatory lipids including DAG (2, 3). Although the generation of vacuolar DAG through the hydrolysis of phosphatidylinositol 4,5-bisphosphate by Plc1p has been demonstrated, the production of DAG through the dephosphoryl-

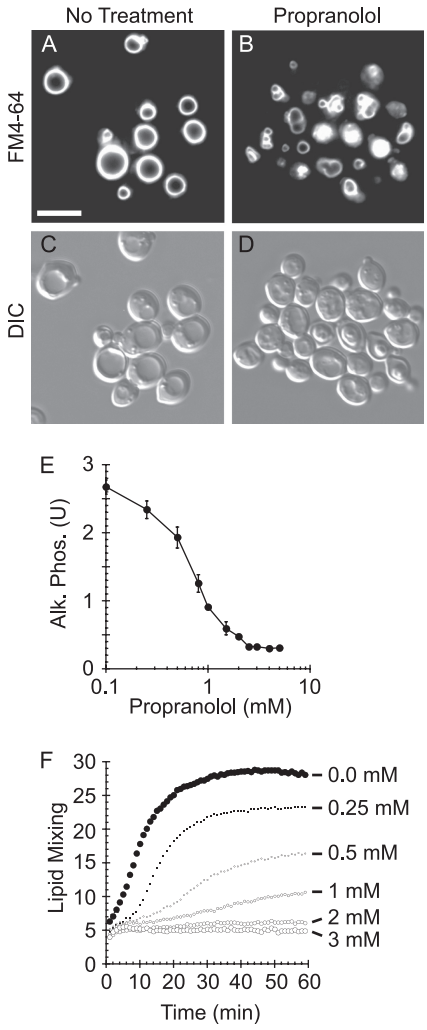

FIGURE 1. **Inhibition of PA phosphatase activity causes vacuole fragmentation and inhibits fusion.** Wild type yeast cells were incubated with 5 μM FM4-64 to label vacuoles. Wild type cells were treated with buffer (*A* and *C*) or 2 mM propranolol (*B* and *D*). Cells were photographed using differential interference contrast (*DIC*), and FM4-64 images were acquired using a 42 HE CY3 shift-free filter set. *Bar*, 5 μM. *E*, vacuoles were harvested from WT BJ3505 (*PHO8 pep4*Δ) and DKY6281 (*pho8*Δ *PEP4*) and tested for fusion by content mixing and proPho8p maturation. Fusion reactions containing 3 μg of each vacuole type were incubated in the absence or presence of the indicated propranolol concentrations. *Alk. Phos.*, alkaline phosphatase. *Error bars* represent S.E. ($n = 3$). *U*, units. *F*, fusion was examined by a real-time lipid-mixing assay. Donor vacuoles were labeled with Rh-PE at self-quenching concentrations. Labeled donor vacuoles (2 μg) were incubated with 16 μg of unlabeled acceptor vacuoles. Fusion was measured by Rh-PE dequenching. Reactions were treated with buffer or propranolol at the indicated concentrations. The experiment is representative of three trials.

ation of PA during vacuole fusion had not been examined. To test the role of PAP activity in vacuole homeostasis, we treated WT yeast cells with the β-adrenergic receptor antagonist propranolol, a known inhibitor of PAP activity (52, 53). To label vacuoles for fluorescence microscopy, yeast were incubated with the vital dye FM4-64. Unlike untreated WT cells, which contain 1–2 large round vacuoles per cell (Fig. 1, *A* and *C*), yeast treated with propranolol contained fragmented and deformed vacuoles (Fig. 1, *B* and *D*). Because vacuole deformation/fragmentation is indicative of irregular homeostasis, this phenotype suggested that the conversion of PA to DAG played a critical role in regulating vacuole function.

To test whether propranolol inhibited vacuole fusion, we used a content mixing assay as previously described (43). Fusion was measured by the maturation of pro-alkaline phosphatase (proPho8p) by proteinase A (Pep4p). Vacuoles were purified from the reciprocally deleted strains DKY6281 (*PEP4 pho8*Δ) and BJ3505 (*pep4*Δ *PHO8*) and used *in vitro* to measure fusion as described under "Experimental Procedures." We found that propranolol potently inhibited vacuole fusion in a dose-dependent manner (Fig. 1*E*), suggesting that PAP activity was required for vacuole fusion. The concentrations required to inhibit fusion mirrored the IC_{50} values reported for purified mammalian Lipin 1 orthologues (54). To determine whether other β-adrenergic receptor antagonists would affect fusion, we also tested atenolol and acebutolol and found that neither compound affected fusion (not shown), suggesting that propranolol inhibited fusion by directly inhibiting PAP activity and not through nonspecific interactions with the membrane. To validate that the effects of propranolol were not due to the inhibition of the Pho8p detection system, we examined its effect on fusion using a real-time lipid-dequenching assay (55, 56). Vacuoles were labeled with Rh-PE at concentrations that caused self-quenching dimerization of the fluorophore. Rh-PE-labeled vacuoles were incubated with an excess of unlabeled vacuoles and monitored for fluorescence dequenching upon fusion. Fusion reactions were incubated with buffer (Fig. 1*F*, *closed circles*) or propranolol (Fig. 1*F*, *open circles*). Rh-PE dequenching was inhibited by propranolol in a dose-dependent manner that recapitulated the inhibition curve seen in content mixing assays.

Deletion of Lipin 1 Orthologue Pah1p Disrupts Vacuolar Homeostasis—Because propranolol inhibited vacuole fusion, we next sought to determine which of the three yeast PA phosphatases regulated this process. We deleted *DPP1*, *LPP1*, and *PAH1* from our fusion tester strains and examined their vacuolar phenotype using FM4-64. Relative to WT cells (Fig. 2, *A* and *B*) we found that the deletion of either *DPP1* (Fig. 2, *C* and *D*) or *LPP1* (Fig. 2, *E* and *F*) had no effect on vacuole morphology. Importantly, the vacuoles in *pah1*Δ cells (Fig. 2, *G* and *H*) were fragmented and deformed in a manner similar to the effect of propranolol, indicating that Pah1p activity was specifically involved in vacuolar homeostasis.

We next tested *in vitro* fusion using purified vacuoles from WT and *pah1*Δ cells and found that fusion was severely attenuated by the deletion of *PAH1* (Fig. 3*A*). Because the lack of fusion was likely due to the absence of PAP activity, we complimented *pah1*Δ strains with plasmids that expressed either WT *PAH1* or the phosphatase dead mutant $PAH1^{D398E}$ (46). Complementation of *pah1*Δ strains with WT p*PAH1* fully rescued fusion, illustrating that the inhibition in fusion was directly due to the loss of Pah1p (Fig. 3*B*). In contrast, p$PAH1^{D398E}$ did not rescue the null phenotype, demonstrating that Pah1p phosphatase activity was required for vacuole fusion (Fig. 3*C*). We next labeled the vacuoles of WT, *pah1*Δ, and complemented strains with FM4-64. As seen in Fig. 2, WT cells contained 1–2 vacuoles per cell (Fig. 3*D*), whereas *pah1*Δ cells harbored fragmented and deformed vacuoles (Fig. 3*E*). When *pah1*Δ cells were complemented with p*PAH1*, we observed the restoration of WT vacuole morphology (Fig. 3*F*), whereas the expression of

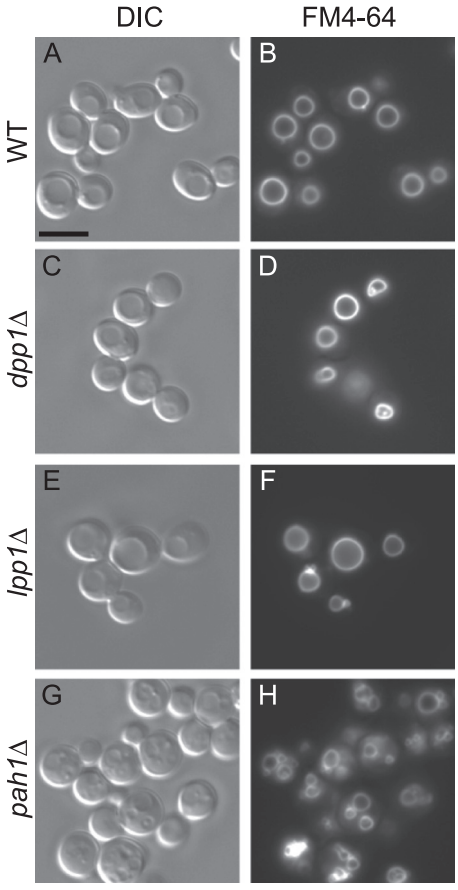

FIGURE 2. **The Lipin 1 orthologue Pah1p is required for vacuolar homeostasis.** Each of the three PA phosphatases (*LPP1*, *DPP1*, and *PAH1*) in *S. cerevisiae* was deleted in individual strains. WT (*A* and *B*), *dpp1*Δ (*C* and *D*), *lpp1*Δ (*E* and *F*), and *pah1*Δ (*G* and *H*) strains were incubated with the lipophilic dye FM4-64 to label vacuoles. Cells were photographed using differential interference contrast, and FM4-64 images were acquired using a 42 HE CY3 shift-free filter set. *Bar*, 5 μM.

p*PAH1*^{D398E} did not affect the fragmentation phenotype (Fig. 3*G*). To verify that changes in fusion using *pah1*Δ strains were not due to the inactivation of the Pho8p/Pep4p reporter system, we also performed lipid-dequenching experiments using *pah1*Δ strains. As seen with the content mixing assay, *pah1*Δ vacuoles were blocked in fusion relative to WT vacuoles (Fig. 3*H*). We also deleted *DPP1* and *LPP1* from our fusion tester strains and found that that *dpp1*Δ and *lpp1*Δ vacuoles fused as well as WT vacuoles (Fig. 3, *I* and *J*, respectively). Together these data demonstrated that only Pah1p played a role in vacuole fusion.

Pah1p Localizes to Vacuole—Because Pah1p is a soluble phosphatase that mostly associates with the endoplasmic reticulum, which in whole cells masks its localization to other organelles, we examined purified vacuoles for the recruitment of this enzyme. To this end we probed for Pah1p on vacuoles by two means. We first used cell fractionation to determine the distribution of Pah1p. Cells expressing Pah1p-HA$_3$ were lysed and fractionated into cytosolic and membranous fractions (microsomes) that included vacuoles. We also tested purified vacuoles from this strain. The cellular fractions were resolved by SDS-PAGE and probed for Pah1p-HA$_3$ or Ypt7p by Western blot. We observed that the majority of the Pah1p was in the cytosolic fractions, whereas a lower amount of Pah1p was observed on microsomes and vacuoles (Fig. 4*A*). Ypt7p was highly enriched on vacuoles and detected at low levels in the lysate and microsome fractions. This indicated that although the majority of the Pah1p was found in the cytosol, a notable concentration of the enzyme was recruited to the vacuole.

In separate experiments, we fused GFP to the C terminus of Pah1p (Pah1p-GFP) to visualize its distribution on isolated vacuoles by microscopy. Purified Pah1p-GFP vacuoles were incubated in docking reactions and observed by wide-field fluorescence microscopy. FM4-64 was used to stain the membrane. We found that Pah1p-GFP was present on the vacuole and evenly distributed across the membrane (Fig. 4*B*). This was not easily observed when examining whole cells by microscopy. The high concentration of Pah1p-GFP in the cytosol masked vacuole-associated protein (not shown). To confirm that Pah1p-GFP was indeed localized to the vacuolar membrane and not due to contaminating debris, we performed deconvolution fluorescence microscopy. Here, Pah1p-GFP vacuoles were co-stained with PSS-380 to label phosphatidylserine (57). Z-series of images were collected of individual vacuoles and deconvolved using Axiovision software. Individual vacuoles were used instead of clusters to eliminate the possible fluorescence contributed by membranous debris. Fig. 4*C* shows central slice images of Pah1p-GFP and PSS-380. We used PSS-380 in lieu of FM4-64 due of its resistance to bleaching during multiple exposures in Z-series acquisition. This further demonstrated that Pah1p-GFP was truly recruited to the vacuolar membrane and not associated with contaminating membranes.

PAP Activity Is Required for SNARE Priming—To determine when PAP activity functions during the fusion pathway, we tested the temporal acquisition of resistance to propranolol (6, 7, 36). As a fusion reaction passes a specific stage, such as Sec18p-dependent priming, it gains resistance to inhibitors that target that particular stage (*e.g.* anti-Sec18p) (6). Here we compared the ability of propranolol or anti-Sec18p antibody to inhibit fusion. Inhibitors were added at fixed concentrations to individual reactions at the indicated times and incubated for a total of 60 min. We found that fusion became resistant to anti-Sec18p (Fig. 5*A*, *open diamonds*) with kinetics similar to previous reports (6, 58, 59). In addition, we found that the acquisition of resistance toward propranolol followed a kinetic curve similar to that of anti-Sec18p (Fig. 5*A*, *open circles*). This strongly suggested that PAP function was only required during the priming stage.

We next examined the release of Sec17p (α-soluble NSF attachment protein) from SNAREs after *cis*-complex disassembly by Sec18p (6). Fusion reactions were incubated with buffer or propranolol for the indicated times followed by centrifugation to collect the vacuole fraction and decanting of the supernatant. Fig. 5*B* shows that Sec17p was released from vacuoles when treated with buffer alone; however, this was blocked in the presence of propranolol, indicating that SNARE priming required PAP activity. As a control for the loss of membranes during re-isolation, we probed for Ypt7p, a membrane-anchored Rab GTPase. Neither treatment affected Ypt7p levels, demonstrating that the loss of Sec17p during priming was not due to a loss of membranes.

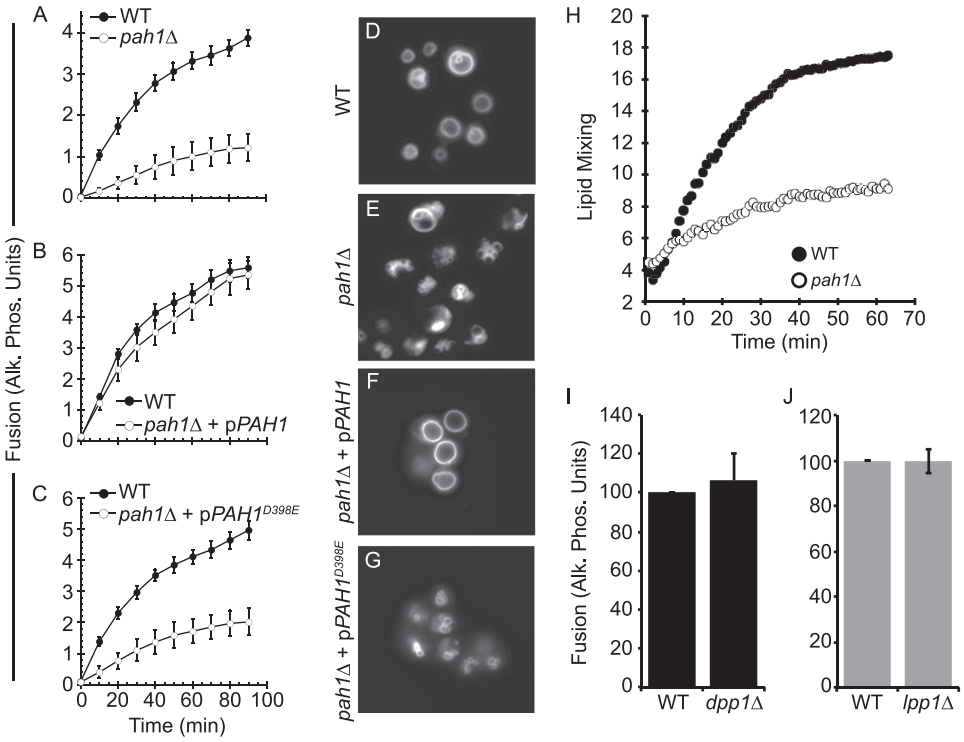

FIGURE 3. **Pah1p is required for vacuole fusion.** *A*, fusion reactions were carried out using WT and *pah1*Δ vacuoles or vacuoles from *pah1*Δ strains complemented with WT p*PAH1* (*B*) or phosphatase dead p*PAH1*^{D398E} (*C*). Fusion reactions were incubated at 27 °C for the indicated times and assayed for proPho8 maturation. *Error bars* represent S.E. ($n = 3$). *D*—*G*, yeast cells (WT, *pah1*Δ, *pah1*Δ + p*PAH1*, *pah1*Δ + p*PAH1*^{D398E}) were incubated with 5 μM FM4-64 to label vacuoles. *H*, fusion was examined by a real-time lipid-mixing assay. WT or *pah1*Δ. Donor vacuoles were labeled with Rh-PE at self-quenching concentrations. Labeled donor vacuoles were incubated with the respective unlabeled acceptor vacuoles as described under "Experimental Procedures." Fusion was measured by Rh-PE dequenching upon outer leaflet mixing. The experiment is representative of three trials. *I–J*, content mixing fusion assays were performed using vacuoles from WT, *dpp1*Δ (I) or *lpp1*Δ (J) strains. *Errors bars* represent S.E. ($n = 3$). *Alk. Phos.*, alkaline phosphatase.

PA Phosphatase Activity Regulates Sec18p-SNARE Binding—Because propranolol inhibition was shown to occur during the priming stage, we next examined the specific binding of Sec18p to SNARE complexes during priming. For these experiments we used vacuoles that harbored Vam3p containing an internal CBP between its regulatory N terminus and SNARE domain (*CBP-VAM3 NYV1*) (44). We monitored the release of Sec18p from SNARE complexes after priming. In untreated reactions, Sec18p was released from SNARE complexes over time as priming occurred (Fig. 5*C*). The release of Sec18p was blocked when priming was inhibited with anti-Sec18p antibody. When reactions were treated with propranolol we observed that Sec18p was sharply reduced at the beginning of the reaction. Fig. 5*D* shows quantitation of Sec18p associated with CBP-Vam3p complexes, suggesting that PAP activity was required for Sec18p association with *cis*-SNARE complexes and that downstream effects were manifest in the slowed rate of priming.

Next, we determined whether propranolol caused a general loss of Sec18p from the entirety of the vacuolar membranes. Fusion reactions were treated with buffer or propranolol, after which membranes were re-isolated by centrifugation and examined for membrane-bound Sec18p by Western blot. We found that Sec18p levels were not affected by propranolol treatment (Fig. 5*E*), suggesting that PAP activity was required for the association of Sec18p with *cis*-SNARE complexes and that Sec18p also binds vacuolar membranes independent of SNARE proteins. Importantly, the mammalian Sec18p homologue NSF has been shown to specifically bind PA (60); thus, we posit that PA phosphatase activity may lead to the release of membrane-bound pools of NSF/Sec18p and recruitment to *cis*-SNARE complexes.

Propranolol Inhibits Endogenous Vacuole PAP Activity during Fusion—To determine whether propranolol inhibited PAP activity on vacuoles, we next examined native PAP activity during fusion. We used thin layer chromatography and NBD-tagged PA to monitor the production of NBD-DAG. Short chain Di-C6-NBD PA was incubated with vacuoles and treated with propranolol. Lipids were extracted and resolved by TLC as described under "Experimental Procedures." A clear NBD-DAG spot was produced when vacuoles were incubated with NBD-PA, indicating that vacuoles exhibited PAP activity during membrane fusion (Fig. 5, *F* and *G*). Increasing concentrations of propranolol inhibited DAG production, illustrating a positive correlation between the inhibitions of fusion and PAP activity.

Vam7p Bypasses Propranolol Block and Rescues Fusion—Because propranolol inhibited SNARE priming, we hypothesized that the block could be bypassed with exogenous Vam7p, a soluble SNARE that can bypass an anti-Sec17p priming block by interacting with free SNAREs to form fusogenic *trans*-SNARE complexes (40, 41, 61). Accordingly, we found that fusion was restored when propranolol-treated vacuoles were incubated with WT Vam7p (Fig. 6*A*). Strikingly, we also found that fusion was restored with Vam7p containing a mutation in the ionic zero layer of the SNARE domain (Vam7p^{Q283R}). Dis-

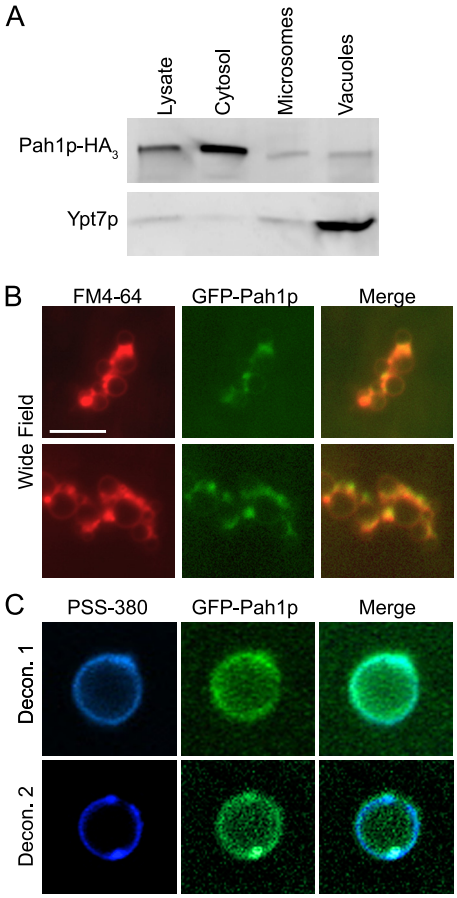

FIGURE 4. **Pah1p localizes to the vacuole membrane.** *A*, samples were isolated from WT DKY6281 and Pah1p-HA strains. Western blots were performed on whole cell lysate, cytosol, a microsomal fraction, and purified vacuoles. Each *lane* contained 10 μg of protein for lysate, cytosol, and microsome samples or 30 μg of vacuoles. Microsomes and lysates were prepared as described previously (49). Antibody against HA was used to detect Pah1p-HA, and anti-Ypt7p was used to detect the vacuolar Rab GTPase. *B*, vacuoles harboring Pah1p-GFP were used for fluorescence microscopy. Vacuoles were incubated for 30 min under docking conditions, co-stained with FM4-64, and mounted for wide-field fluorescence microscopy examination. *Bar*, 10 μm. *C*, Z-stacks of images were taken of individual Pah1p-GFP vacuoles incubated under docking conditions for 30 min. Vacuoles were co-stained with 1 μM PSS-380 to label phosphatidylserine. Images were deconvolved using AxioVison 3D software. Shown are the center slices of two separate z-stacks of independent vacuoles.

rupting the 3Q:1R paradigm with Vam7p^{Q283R} (2Q:2R) abolishes vacuole fusion unless vacuoles are treated with agents that increase membrane fluidity (41). We theorized that increasing membrane fluidity lowers the energy threshold required for SNARE complexes to deform membranes and mediate fusion. Others have found that propranolol in addition to other β-blockers increase the fluidity of biomimetic liposomes (62); thus, the activity of Vam7p^{Q283R} SNARE complexes in the presence of propranolol was in accord with our previous findings linking fluidity to the function of Vam7p^{Q283R}. However, it must be noted that other β-blockers that alter membrane fluidity did not alter vacuole fusion. In addition, the effect of propranolol only altered fusion at the priming stage. The acquisition of resistance seen above was indicative that the drug did not cause nonspecific changes to the membrane. Unlike the SNARE domain mutation, a Phox homology domain mutation (Vam7p^{Y42A}) that blocks PI3P binding did not rescue fusion. This was consistent with our prior finding showing that Vam7p^{Y42A} could not bypass priming blocked with anti-Sec17p IgG (40) and was likely due to the stringent requirement for PI3P-binding by Vam7p.

To verify that the Vam7p (WT and Q283R) bypass of propranolol-blocked fusion was dependent on the endogenous fusion machinery, we used inhibitors that block fusion upstream and downstream of Vam7p binding. We found that Vam7p bypass was sensitive to antibodies against the SNARE Vam3p and the HOPS subunit Vps33p (Fig. 6*B*). Both Vam3p and Vps33p are essential for Vam7p bypass activity (61). Antibodies against the Rab GTPase Ypt7p and Sec18p did not inhibit Vam7p bypass, which was in accord with the notion that Vam7p stimulates fusion at the docking stage, downstream of Sec18p-dependent priming and reversible Rab-mediated tethering.

Propranolol Inhibits trans-SNARE Complex Formation—To confirm that PAP activity was required early during the fusion pathway, we examined a downstream event that required *cis*-SNARE priming. Here we tested whether *trans*-SNARE complexes would form when PAP activity was inhibited. The formation of *trans*-SNARE pairs occurs at the docking stage and precedes Ca^{2+} efflux, hemifusion, and full content mixing. We examined the formation of *trans*-SNARE pairs by monitoring the formation of Vam3p-Nyv1p complexes (44, 50). To ensure that Vam3p and Nyv1p were in *trans*, we used vacuoles harvested from two different strains. Vacuoles from one strain lacking Nyv1p and harboring CBP-Vam3p (*CBP-VAM3 nyv1*Δ) were incubated with WT vacuoles (*VAM3 NYV1*) and allowed to form *trans*-SNARE pairs that contained CBP-Vam3p from one vacuole and Nyv1p from the partner vacuole. We treated the reactions with propranolol, Vam7p alone or inhibitors that block *trans*-SNARE pairing. MED was used to bind phosphoinositides (2), and Ypt7p function was inhibited with a mixture of the Rab GTPase activating protein Gyp1p and Rab GDP dissociation inhibitor (61). Treatment with propranolol blocked the formation of *trans*-SNARE pairing as shown by the absence of Nyv1p in isolated CBP-Vam3p complexes (Fig. 6*C*, *lane 11*) relative to untreated reactions (Fig. 6*C*, *lane 7*). CBP-Vam3p bound ~0.6% of the Nyv1p from the acceptor vacuoles when reactions were treated with buffer alone and was reduced to 0.2% when treated with propranolol (Fig. 6*D*, *gray bars*). It should be noted that WT vacuoles also fuse with themselves, leading to reduced levels of Nyv1p available to complex with CBP-Vam3p. The inhibition of *trans*-SNARE formation and fusion by propranolol was as robust as the characterized inhibitors MED and Gyp1/Rab GDP dissociation inhibitor (*GDI*) (Fig. 6*C*, *lanes 9* and *10*, respectively, and Fig. 6*D*). The addition of recombinant GST-Vam7p enhanced the formation of *trans*-SNARE complexes in untreated reactions (Fig. 6*C*, *lane 8*) without affecting the extent of fusion (Fig. 6*D*, *black bars*). However, when GST-Vam7p was added to propranolol-treated reactions, it restored *trans*-SNARE pairing as well as fusion (Fig. 6, *C*, *lane 12*, and *D*). These data are in agreement with the inhibition of priming by propranolol. Furthermore, this demonstrated that the fusion machinery itself was fully operational, as shown by the ability of Vam7p to bypass the propranolol block.

*Vam7p Does Not Rescue pah1*Δ *Vacuole Fusion*—Because the propranolol block was bypassed by the addition of exogenous

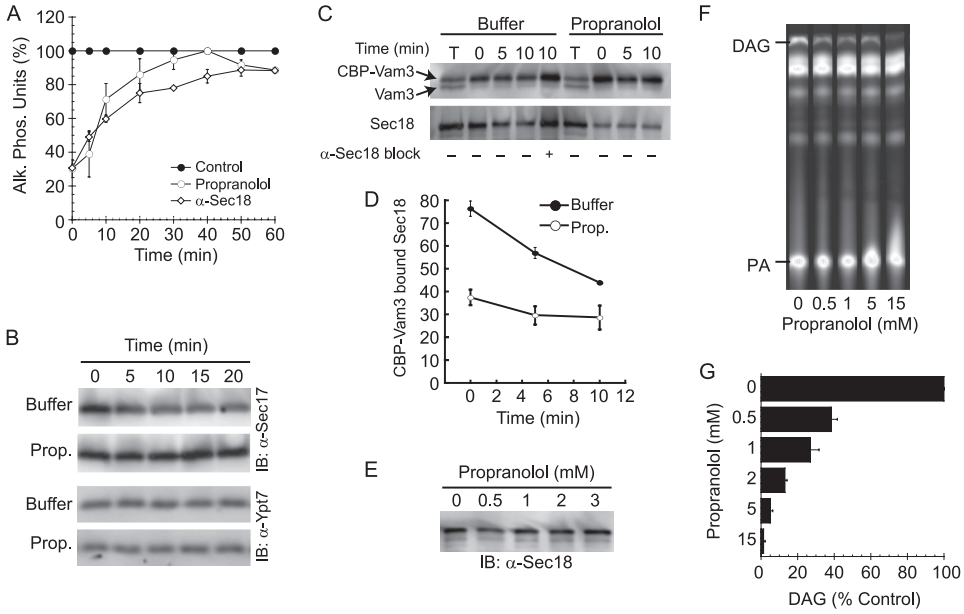

FIGURE 5. **Propranolol inhibits fusion during the priming stage.** *A*, individual fusion reactions were treated with buffer, 1 μg/ml anti-Sec18p, or 2 mM propranolol at the indicated time points. At the end of 60 min, all reactions were assayed for Pho8p activity. *Alk. Phos.*, alkaline phosphatase. *B*, priming was tested by the release of Sec17p from the membrane fraction. Fusion reactions were treated with buffer or 2 mM propranolol (*Prop.*) and incubated for the indicated times. Vacuoles were reisolated by centrifugation (13,000 × *g*, 15 min, 4 °C), resuspended in SDS-loading buffer, resolved by SDS-PAGE, and transferred to nitrocellulose. Western blots (*IB*) were performed using antibody against Sec17p or membrane anchored Ypt7p. *C*, to examine the dissociation of Sec18p from *cis*-SNARE complexes, we monitored the binding of Sec18p to isolated CBP-Vam3p complexes. Vacuoles harboring CBP-Vam3p (*NYV1 CBP-VAM3*) were incubated at 27 °C for the indicated times in the presence or absence of 2 mM propranolol. An additional reaction was treated with anti-Sec18p to inhibit priming. After incubation, reactions were centrifuged to isolate the membrane fraction. Membranes were solubilized, and CBP-Vam3p complexes were isolated with calmodulin-agarose. Complexes were probed by Western blotting for Vam3p and Sec18p. The experiment shown is representative of three trials. *The first* and *sixth lanes* contain 10% of the total reaction (*T*). *D*, shown is quantitation of Sec18p bound to CBP-Vam3p. Values represent concentrations (%) relative to the 10% input. *Error bars* represent S.E. ($n = 3$). *E*, fusion reactions were treated with the indicated concentrations of propranolol. After incubation (10 min, 27 °C) the membrane fraction was collected by centrifugation (13,000 × *g*, 10 min, 4 °C). After discarding the supernatant, the membrane pellets were suspended in SDS-PAGE buffer, boiled for 5 min, and resolved by SDS-PAGE. Sec18p levels were examined by Western blot. *F*, fusion reactions were incubated in the presence of NBD-labeled PA. After 30 min, lipids were extracted and resolved by TLC. Generation of NBD-DAG was detected using phosphorimaging. *G*, relative concentrations of NBD-DAG were calculated in the presence and absence of propranolol. *Error bars* represent S.E. ($n = 3$).

Vam7p, we next tested if the soluble SNARE would also bypass the *pah1*Δ defect. Fusion reactions containing either WT or *pah1*Δ vacuoles were treated with buffer or anti-Sec17p to block priming, after which recombinant Vam7p was added to restore fusion. As previously reported, the addition of Vam7p bypassed the priming block of WT vacuoles treated with anti-Sec17p (Fig. 7*A*). Interestingly, Vam7p did not rescue the fusion of *pah1*Δ vacuoles, which suggested that deleting the Pah1p phosphatase might block fusion by a mechanism other than priming.

To further investigate the inability of Vam7p to rescue the fusion block of *pah1*Δ vacuoles, we performed GST-Vam7p pulldown experiments to examine protein interactions. As a control, we used WT vacuoles to test the binding of GST-Vam7p to other SNAREs and the HOPS complex. In Fig. 7*B* we show that in WT fusion reactions GST-Vam7p formed isolable complexes with the SNARE Vam3p as well as the HOPS subunits Vps16p and Vps33p. Antibody against Vam3p blocked complex formation with Vam7p but had no effect on HOPS binding. When the same experiment was performed with *pah1*Δ vacuoles, we found that Vam7p was unable to form stable complexes with Vam3p or HOPS. In addition, the total amount of Vam7p associated with the membrane in the 10% sample load was reduced on *pah1*Δ vacuoles (Fig. 7*B*, *lane 7*), which indicated that Vam7p was less able to associate with the membrane. Importantly, the endogenous levels Vam3p and HOPS subunits were reduced on *pah1*Δ vacuoles relative to WT vacuoles (Fig. 7*B*, *lanes 1* and 7). Together these data suggested that the deletion Pah1p altered the recruitment/trafficking of fusion regulators to the vacuole.

Pah1p Regulates Sorting of Fusion Factors to Vacuole—Because of the reduction of fusion regulators observed in Fig. 7*B*, we further characterized *pah1*Δ vacuoles by Western blotting. We found that the mutant vacuoles had reduced concentrations of additional trafficking effectors. Importantly, *pah1*Δ vacuoles were nearly devoid of the phosphoinositide 3-kinase Vps34p and the late endosomal Rab Ypt7p as well as Vps39p, a HOPS subunit indirectly associated with the recruitment of Ypt7p to the vacuole (Fig. 8*A*). The reduction in HOPS and Vam7p was likely due to the absence of Ypt7p and the lipid PI3P, a product of Vps34p activity. Although a critical group of fusion regulators was reduced on *pah1*Δ vacuoles, it is important to note that other factors were not affected. For example, the levels of actin, the R-SNARE Ykt6p, and Sec18p were not affected by deleting *PAH1*. Importantly, the trafficking of Pho8p and Pep4p were also not affected by the deletion of *PAH1*, demonstrating that the AP-3 and carboxypeptidase Y biosynthetic pathways to the vacuole were intact and suggested that the reduction of some proteins was not due to the overall shutdown of trafficking pathways to the vacuole. However, this does not exclude the possibility that some cargo was mispackaged into transport vesicles destined for the vacuole, which is

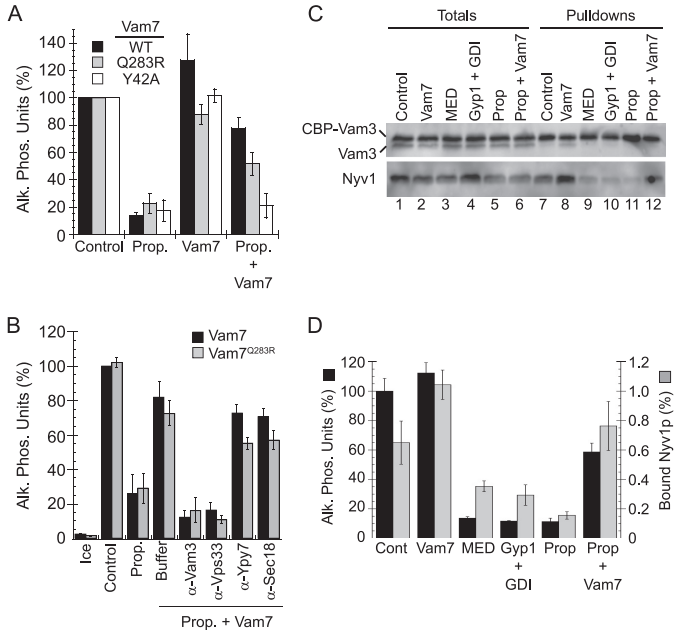

FIGURE 6. **Vam7p bypasses the propranolol-induced priming block.** *A*, fusion reactions were incubated with buffer alone, 2 mM propranolol (*Prop.*), 400 nM Vam7p (WT, Q283R, or Y42A), or propranolol and Vam7p together. Reactions were incubated for 90 min and examined for fusion. *Alk. Phos.*, alkaline phosphatase. *B*, to test whether the Vam7p bypass was on the pathway, fusion reactions were incubated with buffer or 2 mM propranolol in the presence or absence of Vam7p (WT or Q283R). In a subset of bypass reactions, antibodies were added against Vam3p, Vps33p, Ypt7p, or Sec18p before adding Vam7p. Reactions were incubated for 90 min and assayed for fusion. *C*, for the isolation of *trans*-SNARE complexes, vacuoles lacking Nyv1p and harboring CBP-Vam3p (*nyv1*Δ *CBP-VAM3*) were incubated with DKY6271 vacuoles (*NYV1 VAM3*). Reactions were treated with 2 mM propranolol or known inhibitors of *trans*-SNARE pairing (10 μM MED or 0.5 μm Gyp1 + 0.5 μM Rab GDP dissociation inhibitor (*GDI*)). Separate propranolol-treated reactions were incubated with 400 nM Vam7p. Reactions were incubated at 27 °C for 60 min. After incubating, reactions were placed on ice for 5 min, and 30 μl was withdrawn from each reaction to assay fusion. The membrane fraction was isolated by centrifugation and suspended with solubilization buffer containing protease inhibitors. CBP-Vam3p complexes were isolated with calmodulin-Sepharose, resolved by SDS-PAGE, and probed for Vam3p and Nyv1p by Western blotting. *D*, quantitation of fusion and efficiency of Nyv1p binding to CBP-Vam3p are shown. *Error bars* represent S.E. ($n = 3$).

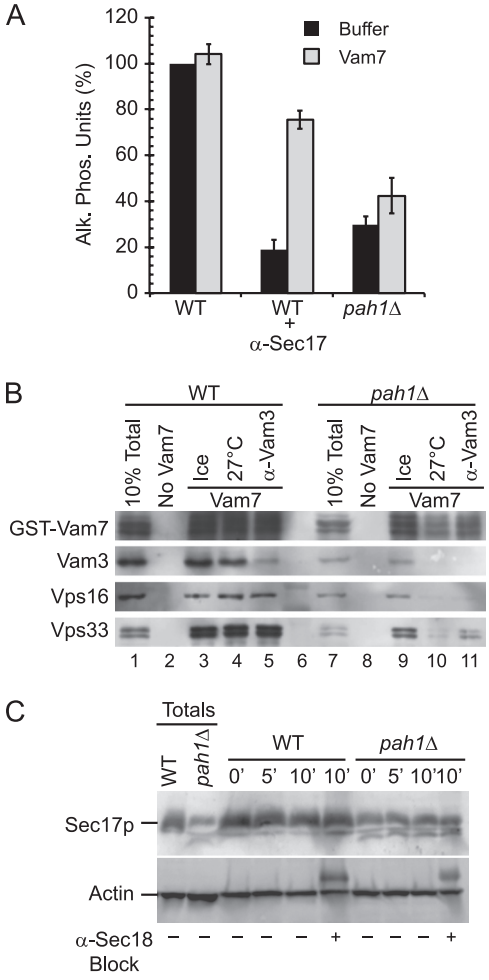

FIGURE 7. **Vam7p does not rescue the *pah1*Δ fusion defect.** *A*, fusion reactions containing WT or *pah1*Δ vacuoles were treated with buffer or anti-Sec17p antibody to block SNARE priming. Fusion reactions were also treated with the recombinant 400 nM GST-Vam7p to bypass the priming block. *Alk. Phos.*, alkaline phosphatase. *B*, SNARE complex formation was tested using WT and *pah1*Δ vacuoles. Fusion reactions were treated with anti-Sec17 antibody to inhibit SNARE priming. GST-Vam7p (400 nM) was added to bypass the priming block. A subset of reactions was treated with anti-Vam3 antibody to block the Vam7p bypass. GST-Vam7p protein complexes were isolated as described under "Experimental Procedures" and analyzed by immunoblotting using antibodies against Vam7p, Vam3p, Vps11p, and Vps33p.

illustrated by the disparate sorting of individual vacuolar SNAREs. Although the vacuolar SNAREs Vam3p, Vti1p, and Nyv1p are all transported to the vacuole via the AP-3 pathway, *pah1*Δ vacuoles were unevenly depleted in these SNAREs, with the sharpest decrease seen in Nyv1p sorting. At this time it is unclear how the lack of Pah1p leads to this disparity.

When *pah1*Δ strains were complemented with plasmid-encoded WT *PAH1*, the vacuolar concentration of all the tested proteins was restored to WT levels, whereas complementation with the phosphatase dead mutant $PAH1^{D398E}$ had no effect on the null phenotype. This demonstrated that the phosphatase activity of Pah1p was required for trafficking/recruiting key proteins to the vacuole. It is important to note that HOPS, Vam7p, and Vps34p are soluble proteins that are recruited from the cytosol to vacuoles by membrane-anchored proteins and lipids. In addition, although Ypt7p is anchored in the vacuole membrane through its geranylgeranyl lipid group, it is recruited from the cytoplasm to maturing endocytic membranes and not sorted through a biosynthetic pathway. To determine whether the absence of soluble or lipid anchored proteins from *pah1*Δ vacuoles was due to defective recruitment or degradation, we examined the levels of Vps34p, Vps39p, and Ypt7p on total membrane fractions. We found that protein levels were not reduced as a whole in *pah1*Δ cells and were present on other membranes. This illustrated that the lack of fusion effectors on *pah1*Δ vacuoles was due to faulty recruitment and not degradation (Fig. 8*B*).

Prolonged Propranolol Treatment Causes Ypt7p Mislocalization—In these experiments we have found that deleting *PAH1* caused a defect in the recruitment of fusion factors from the cytoplasm, including Ypt7p, whereas treatment with propranolol had no great effect on the protein profile of vacuoles. In both cases PA phosphatase activity was targeted in the *in vitro* fusion reaction. However, it must be noted that the inhibition of fusion with propranolol was the result of an acute treatment that occurred after vacuoles had been isolated from WT cells. Thus, the freshly isolated vacuoles were replete with

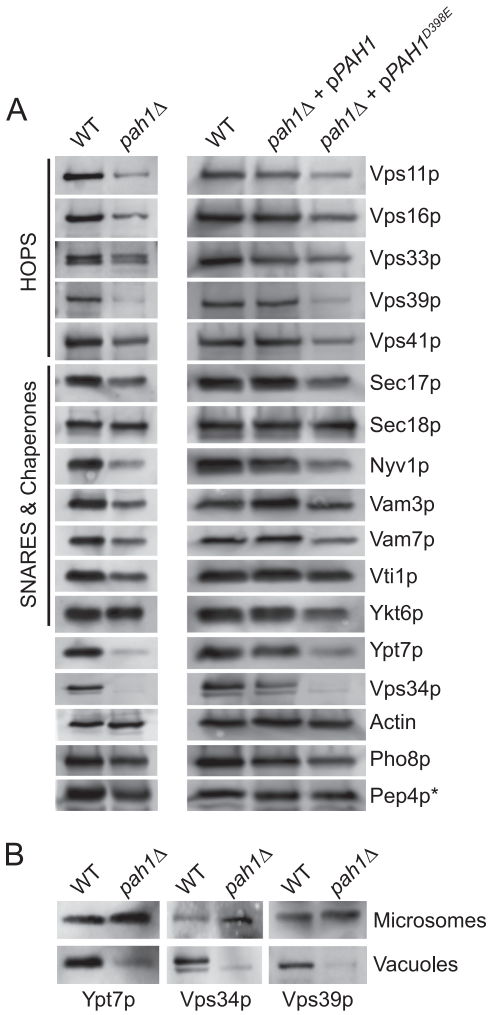

FIGURE 8. **Deletion of *PAH1* alters vacuole homeostasis.** *A*, to analyze the effects of deleting Pah1p on the core fusion machinery, Western blots were performed on vacuoles isolated from WT BJ3505, RFY17 (*pah1*Δ), RFY19 (*pah1*Δ + p*PAH1*), and RFY21 (*pah1*Δ + p$PAH1^{D398E}$) cells. Vacuoles were solubilized with 2× loading buffer, resolved by SDS-PAGE, transferred to nitrocellulose, and probed with antibodies against the indicated proteins. Protein bands were detected using enhanced chemifluorescence. *, to examine the effect of deleting *PAH1* on Pep4p trafficking, vacuoles were isolated from DKY6281 and RFY18, RFY20, and RFY22. *B*, samples were isolated from WT and *pah1*Δ strains, and Western blots were performed on microsomes and purified vacuoles. Microsomes were prepared as previously described (49).

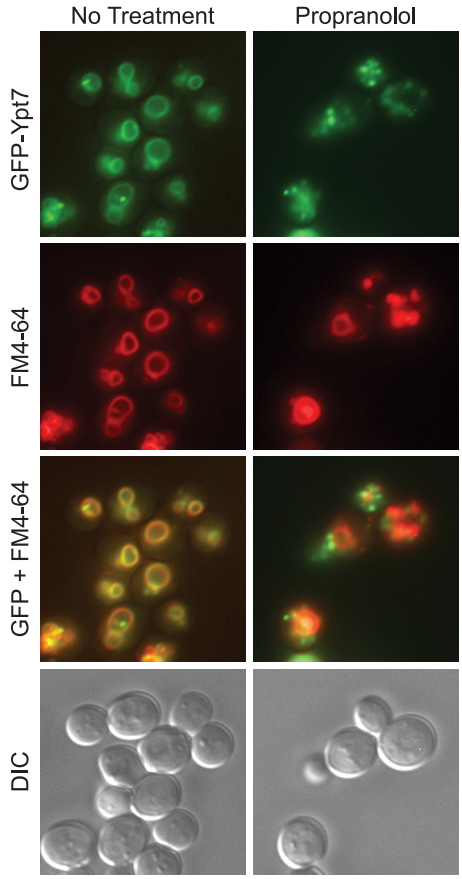

FIGURE 9. **Propranolol treatment caused the missorting of GFP-Ypt7p.** Yeast cells expressing GFP-Ypt7p were grown in YPD and treated with buffer or propranolol for 12 h. Next, the vacuoles were pulse-labeled with FM4-64 for 1 h, washed with PBS, and chased with fresh YPD with or without propranolol for 3 h. After the chase, the cells were washed with PBS and prepared for observation by fluorescence microscopy. GFP-Ypt7p, FM4-64, and differential interference contrast (*DIC*) images were acquired separately. The GFP and FM4-64 images were merged using Photoshop.

the factors necessary for fusion before exposure to propranolol. On the other hand, vacuoles isolated from *pah1*Δ cells reflected the effects of a chronic lack of Pah1p activity.

We next determined whether an extended treatment of intact cells with propranolol would alter protein recruitment to the vacuole. Yeast cells expressing GFP-Ypt7p were treated with buffer or propranolol for 12 h. Vacuoles were next labeled with FM4-64 and examined by fluorescence microscopy. In WT cells GFP-Ypt7p colocalized with FM4-64 at the vacuole as previously reported (12) (Fig. 9). Inhibition of PAP activity caused the mislocalization of GFP-Ypt7p to other endocytic membranes and appeared as large puncta that did not overlap with FM4-64. This indicates that extended treatment with propranolol caused a protein-sorting defect similar to what was seen in *pah1*Δ cells. It is also possible that Ypt7p was recruited and retained to the prevacuolar compartment. These puncta were not representative of a Class E phenotype, as they did not retain FM4-64 in vacuole-adjacent puncta.

*PI3P Is Absent from pah1*Δ *Vacuoles*—Because Vps34p was depleted on *pah1*Δ vacuoles, we predicted that PI3P would be absent or at very low levels in the absence of the kinase. PI3P is made during the vacuole fusion reaction and can be monitored by labeling the lipid with fluorescent FYVE domain (2, 3, 38). Depletion or ligation of PI3P on vacuoles with either high concentrations of FYVE or the PI3P 3-phosphatase MTM-1 blocks vacuole fusion (2, 5); thus, the lack of Vps34p and subsequent PI3P production on *pah1*Δ vacuoles may be a prime mechanism for its abolished fusion.

PI3P accumulates at the vertex ring microdomain and is central in the assembly of fusion factors at this domain (2). To probe for the presence of PI3P on WT or *pah1*Δ vacuoles, we used Cy5-labeled FYVE domain at non-inhibitory concentrations (2, 63). Vacuoles were incubated under docking conditions for 30 min and prepared for fluorescence microscopy examination. Vacuoles were co-stained with FM4-64. As previously reported, we found that WT vacuoles accumulated Cy5-FYVE and, hence, PI3P at vertex ring sites, indicating that Vps34p produced PI3P (Fig. 10, *A* and *B*). In contrast, Cy5-

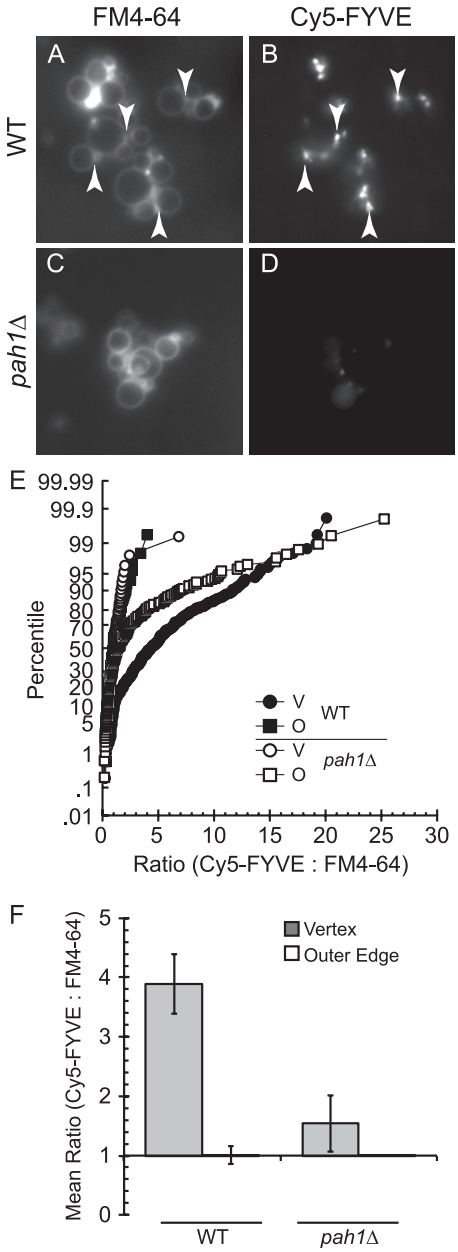

FIGURE 10. **PI3P is absent from *pah1*Δ vacuoles.** *A–D*, vacuoles purified from WT or *pah1*Δ were incubated under docking conditions for 30 min at 27 °C with 0.2 μM Cy5-FYVE. After incubation, vacuoles were stained with FM4-64, mixed with agarose, and prepared for fluorescence microscopy observation. *Arrows* are examples of vertex sites. *E*, cumulative distribution plots show the percentile values of Cy5-FYVE to FM4-64 ratios for each vertex (*V*) and outer edge (*O*). Each curve is compiled from at least 10 vacuole clusters where the maximum pixel intensity was determined for every vertex and midpoint of the outer edge membrane. Pixel intensities were measured in both fluorescence channels at each subdomain and expressed as a ratio of Cy5-FYVE to FM4-64. Outer edge ratios were normalized to a value of 1, and the enrichment of Cy5-FYVE at vertices were expressed relative to outer edge intensities. Each ratio in a dataset is ordered and plotted *versus* the percentile rank of the values. *F*, geometric means with their 95% confidence intervals for the data are in *E*.

FYVE labeling was severely reduced on *pah1*Δ vacuoles (Fig. 10, *C* and *D*), which was consistent with the lack of Vps34p on these vacuoles.

To quantitate the enrichment of PI3P (Cy5-FYVE) at vertices, we used ratiometric fluorescence microscopy that compared the fluorescence intensity of Cy5-FYVE to FM4-64. The clustering of vacuoles and formation of docking sites leads to a doubling of membrane thickness at contact points. Thus, the effect of membrane doubling at docking junctions must be normalized through the used of ratiometric microscopy. In Fig. 10*E*, we show the ratiometric data for WT and *pah1*Δ vacuoles. Each vertex ratio was plotted in a cumulative distribution plot depicting the percentile values of Cy5-FYVE:FM4–64 ratio for each of the strains. Each ratio in a dataset was ordered and plotted *versus* the percentile rank of the values. The ratios of Cy5-FYVE-enriched vertices on WT vacuoles ranged from 0.6 to a maximum of 20 (Fig. 10*E*, *black circles*), causing a right-shift in the curve relative to the outer edge (Fig. 10*E*, *black squares*). When *pah1*Δ vertices were quantitated, we found that the curve was left shifted (*empty circles*) relative to WT vacuoles, indicating that PI3P was markedly reduced on *pah1*Δ vacuoles. Fig. 10*F* shows the geometric means and 95% confidence intervals for the ratios in Fig. 10*E*. These are lower bounds estimates of vertex enrichment due to asynchronous reactions of individual vacuoles within a cluster.

DISCUSSION

Much is known about the role of proteins such as Rabs and SNAREs in the regulation of membrane fusion; however, the regulation of these proteins by their immediate lipid microenvironment remains unclear. Moreover, the continuous modification of lipids species during the fusion pathway is only beginning to be elucidated. The homotypic fusion of yeast vacuoles requires a set of regulatory lipids that are chemically minor yet have critical roles in promoting fusion. Among the growing list of regulatory lipids are phosphoinositides, ergosterol, and DAG, which are modified through the activity of phosphatases, kinases, and lipases. For instance, DAG can be produced by the hydrolysis of phosphatidylinositol 4,5-bisphosphate by Plc1p and deletion or inactivation of Plc1p inhibits fusion (3). DAG is additionally produced by the dephosphorylation of PA; however, the role of PA phosphatases in the production of DAG was not clear in the context of membrane fusion. PA itself has also been found to be essential for maximal fusion of reconstituted proteoliposomes containing yeast vacuolar SNAREs (15), suggesting that a critical balance between these lipid intermediates may be controlled in conjunction with the SNARE machinery. In this study we examined the role of yeast PA phosphatases in vacuole homeostasis and fusion. We used a pharmacological and genetic approach to determine the effect of PAP activity on fusion. Initially we found that inhibiting PAP activity with the small molecule propranolol inhibited fusion at the priming stage, which was bypassed with the soluble SNARE Vam7p, indicating that the inhibition in fusion was not due to irreversible adverse effects of the drug. In testing the effects of deleting each of the three yeast PA phosphatases, we found that only the Lipin 1 orthologue Pah1p played a role in fusion. Our studies found that the enzymatic activity of Pah1p was essential for fusion to occur. Deletion of Pah1p not only led to an inhibition of SNARE-mediated fusion; it also led to the defective trafficking and recruitment of key fusion regulators to the vacuole membrane including the recruitment and activation of the vacuolar Rab GTPase Ypt7p.

PA Phosphatase Activity and SNARE Priming—Our findings indicate that PA phosphatase activity is required during the priming stage. Inhibiting PAP activity with propranolol resulted in a loss of Sec18p from *cis*-SNARE complexes without affecting the total concentrations of membrane-bound Sec18p. Based on these findings we posit that PA phosphatase activity regulates Sec18p-mediated *cis*-SNARE priming. Because *pah1*Δ vacuoles lacked multiple fusion factors, we were unable to determine whether priming was specifically altered in the deletion strain; however, the results garnered by the use of propranolol is enticing and may shed light on the regulation of the prepriming stage of fusion. Based on these results we envision two models in which PAP activity could affect Sec18p recruitment to SNARE complexes and trigger priming. Recent structural analysis of full-length SNARE complexes showed that *cis*-SNARE complexes contain continuous α-helical structures that extend through the SNARE motif into the linker region and transmembrane domain (64). Thus, it is possible that changes in the lipid bilayer due to PAP activity lead to the allosteric regulation of SNARE complex conformation and subsequent Sec18p engagement of the *cis*-SNARE complex.

In one model PAP activity may alter the influence of the membrane on *cis*-SNARE conformational changes needed to bind and Sec18p. The local lipid environment has been previously reported to regulate SNARE priming. Binding of either ergosterol or phosphatidylinositol 4,5-bisphosphate with small molecule ligands has been shown to inhibit Sec17p release during the priming stage (4, 14). Taken together, it is possible that the assembly of a lipid microdomain may be necessary for the allosteric regulation of the *cis*-SNARE complex and that in the absence of a favorable physical state, the SNAREs adopt a conformation that hinders Sec18p binding.

A second model proposes that Sec18p is bound to the membrane in a PA-dependent manner before priming. This may occur as a direct interaction with PA or indirectly through another factor. PA has been shown to physically bind mammalian NSF (Sec18p) (60); thus, it is possible that PA hydrolysis releases NSF/Sec18p from the membrane, allowing it to bind *cis*-SNARE complexes. This model is accordant with our data showing that propranolol reduced that amount of Sec18p bound to *cis*-SNARE complexes without affecting the total amount of Sec18p on vacuoles.

Does Pah1p Play Role in Rab Conversion and Organelle Maturation?—Deletion of *PAH1* led to a sharp decrease in recruitment of the phosphatidylinositol 3-kinase Vps34p and the HOPS subunit Vps39p. Taken together with the absence of PI3P and Ypt7p, we posit that Pah1p plays a role in vacuole maturation. Endosomal vesicles undergo a highly regulated conversion from early endosomes to late endosomes and lysosomes. This is characterized in part by the exchange of Rab GTPases and their cognate effectors. Although much remains unknown about these mechanisms, several groups have made seminal discoveries regarding the regulation of this transformation (65–68). Ungermann and co-workers (65) recently discovered the endosomal tethering complex CORVET that shares a core of Class C proteins (Vps11p, Vps16p, Vps18p, and Vps33p) with the vacuolar tethering complex HOPS. In addition to the Class C core, CORVET contains Vps8p and Vps3p, whereas HOPS contains Vps41p and Vps39p. Intermediate complexes exist that contain Vps41p and Vps3p (iCORVET) or Vps8p and Vps39p (i-HOPS). Because *pah1*Δ vacuoles lack Vps39p while retaining Vps41p, albeit at reduced levels, it is possible these vacuoles are trapped in an intermediate maturation stage containing iCORVET. The current model proposes that the exchange of CORVET for HOPS could be coupled with the exchange of Vps21p for Ypt7p, where CORVET-containing endosomes harbor Vps21p, and HOPS-containing vacuoles contain Ypt7p. However, this is only a model and needs to be tested. Because *pah1*Δ vacuoles lack Ypt7p, it is thus possible that these organelles are trapped at a Vps21p-containing stage. Rab exchange is linked to the acquisition of Mon1p and Ccz1p, a heterodimer that functions as the guanine nucleotide exchange factor for Ypt7p (69). Although previous works identified Vps39p as the guanine nucleotide exchange factor for Ypt7p (70), it is now proposed that the HOPS subunit is only indirectly involved through the initial binding of Ypt7p. Interestingly, although Ypt7p was absent from *pah1*Δ vacuoles, we found that it was relatively enriched in the total microsomal fraction and localized to vacuole-adjacent membranes, suggesting that in the absence of Pah1p Ypt7p was stably associated with another organelle. Similarly, Vps34p and Vps39p were enriched in the microsomal fraction independent of Pah1p. However, it is unclear whether Vps39p was in a complex with other HOPS subunits.

Pah1p, PI3P, and Rab Conversion—The role of Mon1p in Rab conversion has recently been the center of rigorous exploration (66, 71). Investigators have found that in *Caenorhabditis elegans*, the Mon1p homologue SAND-1 triggers the switch from early-to-late endosomes. The exchange of the early endosomal Rab5/Vps21p for the late endosomal Rab7/Ypt7p occurred through the recruitment of SAND-1/Mon1p and the inactivation of Rab5 (71), promoting the removal Rab5, whereas Rab7 was recruited to the transitioning endosome. In *sand-1*/*mon1*Δ cells, Rab5 remains active and blocks the recruitment of Rab7. Importantly, Mon1p recruitment requires the regulatory lipid PI3P. In our experiments we found that *pah1*Δ vacuoles lack the phosphatidylinositol 3-kinase Vps34p and its product PI3P. However, low levels of PI3P may still traffic to the vacuole from other membranes that harbor Vps34p. Thus, we hypothesize that Pah1p is required for Vps34p recruitment and PI3P production, thus promoting Mon1p binding and the recruitment of Ypt7p.

The mechanism by which Pah1p phosphatase activity leads to the recruitment of Vps34p remains unclear. In mammalian cells hVPS34 is recruited to early endosomes and activated in a Rab5-GTP dependent manner (72). Thus, PI3P is made before the recruitment of SAND-1 and Rab exchange. Unlike the mammalian homologue, yeast Vps34p activity appears to be independent of the early endosome Rab Vps21p. Instead, yeast Vps34p is activated via Gpa1p, the Gα subunit of a plasma membrane heterotrimeric GTPase (73). Monomeric Gpa1p localizes to the endosome and interacts with Vps34p and Vps15p, a myristoylated serine/threonine protein kinase and subunit of the endosomal phosphatidylinositol 3-kinase complex (74). However, it is unclear whether Gpa1p also recruits or activates Vps34p at the vacuole or if once recruited to the endo-

some Vps34p traffics to the vacuole in a Gpa1p-independent manner. Although Gpa1p does traffic to the vacuole, its sorting is dependent on its monoubiquitination by Rsp5p (75) that subsequently targets it for degradation. It is unclear whether Gpa1p monoubiquitination occurs before or after Vps34p activation at the endosome.

Although the link between Pah1p and PI3P production remains unclear at this time, it is quite certain that the lack of this lipid has deleterious effects on the vacuole fusion machinery. Aside from its role in Rab exchange, PI3P is essential for the formation of the vertex microdomain where fusion occurs (2, 12). Modification or ligation of PI3P inhibits the vertex enrichment of SNAREs, Ypt7p, and HOPS as well as ergosterol, DAG, and other phosphoinositides. Moreover, PI3P directly binds to the Phox homology domain of the soluble SNARE Vam7p and to the HOPS complex (5, 9). The formation of 3Q SNARE complexes as well as *trans*-SNARE complexes is also dependent on PI3P (44, 76, 77). Thus it is evident that recruitment of Vps34p is a major function of Pah1p during vacuole fusion, placing the Lipin 1 homologue and the conversion of PA to DAG at the top of a cascade that leads to the activation of SNARE priming and production of PI3P and Ypt7p recruitment.

Acknowledgments—We thank Dr. George Carman for strains and plasmids and Dr. William Wickner for generous gifts of antisera. We also thank Dr. Christian Ungermann, Margarita Cabrera, Dr. Joanna Shisler, and Jennifer Grant for critical reading of the manuscript and helpful discussions.

REFERENCES

1. Jahn, R., and Südhof, T. C. (1999) Membrane fusion and exocytosis. *Annu. Rev. Biochem.* **68,** 863–911 ,
2. Fratti, R. A., Jun, Y., Merz, A. J., Margolis, N., and Wickner, W. (2004) Interdependent assembly of specific regulatory lipids and membrane fusion proteins into the vertex ring domain of docked vacuoles. *J. Cell Biol.* **167,** 1087–1098
3. Jun, Y., Fratti, R. A., and Wickner, W. (2004) Diacylglycerol and its formation by phospholipase C regulate Rab- and SNARE-dependent yeast vacuole fusion. *J. Biol. Chem.* **279,** 53186–53195
4. Kato, M., and Wickner, W. (2001) Ergosterol is required for the Sec18/ATP-dependent priming step of homotypic vacuole fusion. *EMBO J.* **20,** 4035–4040
5. Boeddinghaus, C., Merz, A. J., Laage, R., and Ungermann, C. (2002) A cycle of Vam7p release from and PtdIns 3-P-dependent rebinding to the yeast vacuole is required for homotypic vacuole fusion. *J. Cell Biol.* **157,** 79–89
6. Mayer, A., Wickner, W., and Haas, A. (1996) Sec18p (NSF)-driven release of Sec17p (α-SNAP) can precede docking and fusion of yeast vacuoles. *Cell* **85,** 83–94
7. Haas, A., Scheglmann, D., Lazar, T., Gallwitz, D., and Wickner, W. (1995) The GTPase Ypt7p of *Saccharomyces cerevisiae* is required on both partner vacuoles for the homotypic fusion step of vacuole inheritance. *EMBO J.* **14,** 5258–5270
8. Mayer, A., and Wickner, W. (1997) Docking of yeast vacuoles is catalyzed by the Ras-like GTPase Ypt7p after symmetric priming by Sec18p (NSF). *J. Cell Biol.* **136,** 307–317
9. Stroupe, C., Collins, K. M., Fratti, R. A., and Wickner, W. (2006) Purification of active HOPS complex reveals its affinities for phosphoinositides and the SNARE Vam7p. *EMBO J.* **25,** 1579–1589
10. Ungermann, C., Sato, K., and Wickner, W. (1998) Defining the functions of trans-SNARE pairs. *Nature* **396,** 543–558
11. Merz, A. J., and Wickner, W. (2004) Trans-SNARE interactions elicit Ca^{2+} efflux from the yeast vacuole lumen. *J. Cell Biol.* **164,** 195–206
12. Wang, L., Seeley, E. S., Wickner, W., and Merz, A. J. (2002) Vacuole fusion at a ring of vertex docking sites leaves membrane fragments within the organelle. *Cell* **108,** 357–369
13. Wang, L., Merz, A. J., Collins, K. M., and Wickner, W. (2003) Hierarchy of protein assembly at the vertex ring domain for yeast vacuole docking and fusion. *J. Cell Biol.* **160,** 365–374
14. Mayer, A., Scheglmann, D., Dove, S., Glatz, A., Wickner, W., and Haas, A. (2000) Phosphatidylinositol 4,5-bisphosphate regulates two steps of homotypic vacuole fusion. *Mol. Biol. Cell* **11,** 807–817
15. Mima, J., and Wickner, W. (2009) *Complex lipid requirements for SNARE- and SNARE chaperone-dependent membrane fusion. J. Biol. Chem.* ***284,*** *27114-27122*
16. Fernández-Ulibarri, I., Vilella, M., Lázaro-Diéguez, F., Sarri, E., Martínez, S. E., Jiménez, N., Claro, E., Mérida, I., Burger, K. N., and Egea, G. (2007) Diacylglycerol is required for the formation of COPI vesicles in the Golgi-to-ER transport pathway. *Mol. Biol. Cell* **18,** 3250–3263
17. Asp, L., Kartberg, F., Fernandez-Rodriguez, J., Smedh, M., Elsner, M., Laporte, F., Bárcena, M., Jansen, K. A., Valentijn, J. A., Koster, A. J., Bergeron, J. J., and Nilsson, T. (2009) Early stages of Golgi vesicle and tubule formation require diacylglycerol. *Mol. Biol. Cell* **20,** 780–790
18. Coluccio, A., Malzone, M., and Neiman, A. M. (2004) Genetic evidence of a role for membrane lipid composition in the regulation of soluble NEM-sensitive factor receptor function in *Saccharomyces cerevisiae*. *Genetics* **166,** 89–97
19. Liu, S., Wilson, K. A., Rice-Stitt, T., Neiman, A. M., and McNew, J. A. (2007) *In vitro* fusion catalyzed by the sporulation-specific t-SNARE light-chain Spo20p is stimulated by phosphatidic acid. *Traffic* **8,** 1630–1643
20. Choi, S. Y., Huang, P., Jenkins, G. M., Chan, D. C., Schiller, J., and Frohman, M. A. (2006) A common lipid links Mfn-mediated mitochondrial fusion and SNARE-regulated exocytosis. *Nat. Cell Biol.* **8,** 1255–1262
21. Humeau, Y., Vitale, N., Chasserot-Golaz, S., Dupont, J. L., Du, G., Frohman, M. A., Bader, M. F., and Poulain, B. (2001) A role for phospholipase D1 in neurotransmitter release. *Proc. Natl. Acad. Sci. U.S.A.* **98,** 15300–15305
22. Toke, D. A., Bennett, W. L., Oshiro, J., Wu, W. I., Voelker, D. R., and Carman, G. M. (1998) Isolation and characterization of the *Saccharomyces cerevisiae* LPP1 gene encoding a Mg^{2+}-independent phosphatidate phosphatase. *J. Biol. Chem.* **273,** 14331–14338
23. Han, G. S., Johnston, C. N., Chen, X., Athenstaedt, K., Daum, G., and Carman, G. M. (2001) Regulation of the *Saccharomyces cerevisiae* DPP1-encoded diacylglycerol pyrophosphate phosphatase by zinc. *J. Biol. Chem.* **276,** 10126–10133
24. Han, G. S., Wu, W. I., and Carman, G. M. (2006) The *Saccharomyces cerevisiae* lipin homolog is a Mg^{2+}-dependent phosphatidate phosphatase enzyme. *J. Biol. Chem.* **281,** 9210–9218
25. Péterfy, M., Phan, J., Xu, P., and Reue, K. (2001) Lipodystrophy in the fld mouse results from mutation of a new gene encoding a nuclear protein, lipin. *Nat. Genet.* **27,** 121–124
26. Suviolahti, E., Reue, K., Cantor, R. M., Phan, J., Gentile, M., Naukkarinen, J., Soro-Paavonen, A., Oksanen, L., Kaprio, J., Rissanen, A., Salomaa, V., Kontula, K., Taskinen, M. R., Pajukanta, P., and Peltonen, L. (2006) Cross-species analyses implicate Lipin 1 involvement in human glucose metabolism. *Hum. Mol. Genet.* **15,** 377–386
27. Loos, R. J., Rankinen, T., Pérusse, L., Tremblay, A., Després, J. P., and Bouchard, C. (2007) Association of Lipin 1 gene polymorphisms with measures of energy and glucose metabolism. *Obesity* **15,** 2723–2732
28. Phan, J., and Reue, K. (2005) Lipin, a lipodystrophy and obesity gene. *Cell Metab.* **1,** 73–83
29. Carman, G. M., and Han, G. S. (2009) Phosphatidic acid phosphatase, a key enzyme in the regulation of lipid synthesis. *J. Biol. Chem.* **284,** 2593–2597
30. Choi, H. S., Su, W. M., Morgan, J. M., Han, G. S., Xu, Z., Karanasios, E., Siniossoglou, S., and Carman, G. M. (2011) Phosphorylation of phosphatidate phosphatase regulates its membrane association and physiological functions in *Saccharomyces cerevisiae*. Identification of Ser-602, Thr-723, and Ser-744 as the sites phosphorylated by CDC28 (CDK1)-encoded cyclin-dependent kinase. *J. Biol. Chem.* **286,** 1486–1498
31. Santos-Rosa, H., Leung, J., Grimsey, N., Peak-Chew, S., and Siniossoglou,

S. (2005) The yeast lipin Smp2 couples phospholipid biosynthesis to nuclear membrane growth. *EMBO J.* **24,** 1931–1941
32. Ubersax, J. A., Woodbury, E. L., Quang, P. N., Paraz, M., Blethrow, J. D., Shah, K., Shokat, K. M., and Morgan, D. O. (2003) Targets of the cyclin-dependent kinase Cdk1. *Nature* **425,** 859–864
33. Karanasios, E., Han, G. S., Xu, Z., Carman, G. M., and Siniossoglou, S. (2010) A phosphorylation-regulated amphipathic helix controls the membrane translocation and function of the yeast phosphatidate phosphatase. *Proc. Natl. Acad. Sci. U.S.A.* **107,** 17539–17544
34. Adeyo, O., Horn, P. J., Lee, S., Binns, D. D., Chandrahas, A., Chapman, K. D., and Goodman, J. M. (2011) The yeast lipin orthologue Pah1p is important for biogenesis of lipid droplets. *J. Cell Biol.* **192,** 1043–1055
35. O'Hara, L., Han, G. S., Peak-Chew, S., Grimsey, N., Carman, G. M., and Siniossoglou, S. (2006) Control of phospholipid synthesis by phosphorylation of the yeast lipin Pah1p/Smp2p Mg^{2+}-dependent phosphatidate phosphatase. *J. Biol. Chem.* **281,** 34537–34548
36. Nichols, B. J., Ungermann, C., Pelham, H. R., Wickner, W. T., and Haas, A. (1997) Homotypic vacuolar fusion mediated by t- and v-SNAREs. *Nature* **387,** 199–202
37. Seals, D. F., Eitzen, G., Margolis, N., Wickner, W. T., and Price, A. (2000) A Ypt/Rab effector complex containing the Sec1 homolog Vps33p is required for homotypic vacuole fusion. *Proc. Natl. Acad. Sci. U.S.A.* **97,** 9402–9407
38. Gillooly, D. J., Morrow, I. C., Lindsay, M., Gould, R., Bryant, N. J., Gaullier, J. M., Parton, R. G., and Stenmark, H. (2000) Localization of phosphatidylinositol 3-phosphate in yeast and mammalian cells. *EMBO J.* **19,** 4577–4588
39. Starai, V. J., Jun, Y., and Wickner, W. (2007) Excess vacuolar SNAREs drive lysis and Rab bypass fusion. *Proc. Natl. Acad. Sci. U.S.A.* **104,** 13551–13558
40. Fratti, R. A., and Wickner, W. (2007) Distinct targeting and fusion functions of the Phox homology and SNARE domains of yeast vacuolar Vam7p. *J. Biol. Chem.* **282,** 13133–13138
41. Fratti, R. A., Collins, K. M., Hickey, C. M., and Wickner, W. (2007) Stringent 3Q.1R composition of the SNARE 0-layer can be bypassed for fusion by compensatory SNARE mutation or by lipid bilayer modification. *J. Biol. Chem.* **282,** 14861–14867
42. Jones, E. W., Zubenko, G. S., and Parker, R. R. (1982) PEP4 gene function is required for expression of several vacuolar hydrolases in *Saccharomyces cerevisiae*. *Genetics* **102,** 665–677
43. Haas, A., Conradt, B., and Wickner, W. (1994) G-protein ligands inhibit *in vitro* reactions of vacuole inheritance. *J. Cell Biol.* **126,** 87–97
44. Collins, K. M., and Wickner, W. T. (2007) Trans-SNARE complex assembly and yeast vacuole membrane fusion. *Proc. Natl. Acad. Sci. U.S.A.* **104,** 8755–8760
45. Longtine, M. S., McKenzie, A., 3rd, Demarini, D. J., Shah, N. G., Wach, A., Brachat, A., Philippsen, P., and Pringle, J. R. (1998) Additional modules for versatile and economical PCR-based gene deletion and modification in *Saccharomyces cerevisiae*. *Yeast* **14,** 953–961
46. Han, G. S., Siniossoglou, S., and Carman, G. M. (2007) The cellular functions of the yeast lipin homolog PAH1p are dependent on its phosphatidate phosphatase activity. *J. Biol. Chem.* **282,** 37026–37035
47. Goldstein, A. L., and McCusker, J. H. (1999) Three new dominant drug resistance cassettes for gene disruption in *Saccharomyces cerevisiae*. *Yeast* **15,** 1541–1553
48. *Bähler, J., Wu, J. Q., Longtine, M. S., Shah, N. G., McKenzie, A., 3rd, Steever, A. B., Wach, A., Philippsen, P., and Pringle, J. R.* (1998) Heterologous modules for efficient and versatile PCR-based gene targeting in *Schizosaccharomyces pombe*. *Yeast* **14,** 943–951
49. Qiu, Q. S., and Fratti, R. A. (2010) The Na^+/H^+ exchanger Nhx1p regulates the initiation of *Saccharomyces cerevisiae* vacuole fusion. *J. Cell Sci.* **123,** 3266–3275
50. Jun, Y., and Wickner, W. (2007) Assays of vacuole fusion resolve the stages of docking, lipid mixing, and content mixing. *Proc. Natl. Acad. Sci. U.S.A.* **104,** 13010–13015
51. Trotter, P. J. (2000) A novel pathway for transport and metabolism of a fluorescent phosphatidic acid analog in yeast. *Traffic* **1,** 425–434
52. Morlock, K. R., McLaughlin, J. J., Lin, Y. P., and Carman, G. M. (1991) Phosphatidate phosphatase from *Saccharomyces cerevisiae*. Isolation of 45- and 104-kDa forms of the enzyme that are differentially regulated by inositol. *J. Biol. Chem.* **266,** 3586–3593
53. Pappu, A. S., and Hauser, G. (1983) Propranolol-induced inhibition of rat brain cytoplasmic phosphatidate phosphohydrolase. *Neurochem. Res.* **8,** 1565–1575
54. Han, G. S., and Carman, G. M. (2010) Characterization of the human LPIN1-encoded phosphatidate phosphatase isoforms. *J. Biol. Chem.* **285,** 14628–14638
55. Reese, C., and Mayer, A. (2005) Transition from hemifusion to pore opening is rate-limiting for vacuole membrane fusion. *J. Cell Biol.* **171,** 981–990
56. Reese, C., Heise, F., and Mayer, A. (2005) Trans-SNARE pairing can precede a hemifusion intermediate in intracellular membrane fusion. *Nature* **436,** 410–414
57. Koulov, A. V., Stucker, K. A., Lakshmi, C., Robinson, J. P., and Smith, B. D. (2003) Detection of apoptotic cells using a synthetic fluorescent sensor for membrane surfaces that contain phosphatidylserine. *Cell Death Differ.* **10,** 1357–1359
58. Collins, K. M., Thorngren, N. L., Fratti, R. A., and Wickner, W. T. (2005) Sec17p and HOPS, in distinct SNARE complexes, mediate SNARE complex disruption or assembly for fusion. *EMBO J.* **24,** 1775–1786
59. Eitzen, G., Thorngren, N., and Wickner, W. (2001) Rho1p and Cdc42p act after Ypt7p to regulate vacuole docking. *EMBO J.* **20,** 5650–5656
60. Manifava, M., Thuring, J. W., Lim, Z. Y., Packman, L., Holmes, A. B., and Ktistakis, N. T. (2001) Differential binding of traffic-related proteins to phosphatidic acid- or phosphatidylinositol 4,5-bisphosphate-coupled affinity reagents. *J. Biol. Chem.* **276,** 8987–8994
61. Thorngren, N., Collins, K. M., Fratti, R. A., Wickner, W., and Merz, A. J. (2004) A soluble SNARE drives rapid docking, bypassing ATP and Sec17/18p for vacuole fusion. *EMBO J.* **23,** 2765–2776
62. Mizogami, M., Takakura, K., and Tsuchiya, H. (2010) The interactivities with lipid membranes differentially characterize selective and nonselective beta1-blockers. *Eur. J. Anaesthesiol.* **27,** 829–834
63. Jun, Y., Thorngren, N., Starai, V. J., Fratti, R. A., Collins, K., and Wickner, W. (2006) Reversible, cooperative reactions of yeast vacuole docking. *EMBO J.* **25,** 5260–5269
64. Stein, A., Weber, G., Wahl, M. C., and Jahn, R. (2009) Helical extension of the neuronal SNARE complex into the membrane. *Nature* **460,** 525–528
65. Peplowska, K., Markgraf, D. F., Ostrowicz, C. W., Bange, G., and Ungermann, C. (2007) The CORVET tethering complex interacts with the yeast Rab5 homolog Vps21 and is involved in endo-lysosomal biogenesis. *Dev. Cell* **12,** 739–750
66. Poteryaev, D., Datta, S., Ackema, K., Zerial, M., and Spang, A. (2010) Identification of the switch in early-to-late endosome transition. *Cell* **141,** 497–508
67. Rink, J., Ghigo, E., Kalaidzidis, Y., and Zerial, M. (2005) Rab conversion as a mechanism of progression from early to late endosomes. *Cell* **122,** 735–749
68. Rivera-Molina, F. E., and Novick, P. J. (2009) A Rab GAP cascade defines the boundary between two Rab GTPases on the secretory pathway. *Proc. Natl. Acad. Sci. U.S.A.* **106,** 14408–14413
69. Nordmann, M., Cabrera, M., Perz, A., Bröcker, C., Ostrowicz, C., Engelbrecht-Vandré, S., and Ungermann, C. (2010) The Mon1-Ccz1 complex is the GEF of the late endosomal Rab7 homolog Ypt7. *Curr. Biol.* **20,** 1654–1659
70. Wurmser, A. E., Sato, T. K., and Emr, S. D. (2000) New component of the vacuolar class C-Vps complex couples nucleotide exchange on the Ypt7 GTPase to SNARE-dependent docking and fusion. *J. Cell Biol.* **151,** 551–562
71. Kinchen, J. M., and Ravichandran, K. S. (2010) Identification of two evolutionarily conserved genes regulating processing of engulfed apoptotic cells. *Nature* **464,** 778–782
72. Nielsen, E., Severin, F., Backer, J. M., Hyman, A. A., and Zerial, M. (1999) Rab5 regulates motility of early endosomes on microtubules. *Nat. Cell Biol.* **1,** 376–382
73. Slessareva, J. E., and Dohlman, H. G. (2006) G protein signaling in yeast. New components, new connections, new compartments. *Science* **314,**

1412–1413
74. Kihara, A., Noda, T., Ishihara, N., and Ohsumi, Y. (2001) Two distinct Vps34 phosphatidylinositol 3-kinase complexes function in autophagy and carboxypeptidase Y sorting in *Saccharomyces cerevisiae*. *J. Cell Biol.* **152,** 519–530
75. Torres, M. P., Lee, M. J., Ding, F., Purbeck, C., Kuhlman, B., Dokholyan, N. V., and Dohlman, H. G. (2009) G protein mono-ubiquitination by the Rsp5 ubiquitin ligase. *J. Biol. Chem.* **284,** 8940–8950
76. Xu, H., Jun, Y., Thompson, J., Yates, J., and Wickner, W. (2010) HOPS prevents the disassembly of trans-SNARE complexes by Sec17p/Sec18p during membrane fusion. *EMBO J.* **29,** 1948–1960
77. Xu, H., and Wickner, W. (2010) Phosphoinositides function asymmetrically for membrane fusion, promoting tethering and 3Q-SNARE subcomplex assembly. *J. Biol. Chem.* **285,** 39359–39365